



This is to certify that the
thesis entitled

Light and Heavy Mineral Diagenesis in the
Cambrian Munising Formation

presented by

John Francis Salvino

has been accepted towards fulfillment
of the requirements for

Master's degree in Geology

A handwritten signature in cursive script, reading "Michael Anthony Veltri".

Major professor

Date 5/21/87



3 1293 01103 2640



RETURNING MATERIALS:
Place in book drop to
remove this checkout from
your record. FINES will
be charged if book is
returned after the date
stamped below.

JUL 05 1999

LIGHT AND HEAVY MINERAL DIAGENESIS IN THE
CAMBRIAN MUNISING FORMATION

By

John Francis Salvino

A THESIS

Submitted to
Michigan State University
in partial fulfillment of the requirements
for the degree of

MASTER OF SCIENCE

Department of Geological Sciences

1986

ABSTRACT

LIGHT AND HEAVY MINERAL DIAGENESIS IN THE CAMBRIAN MUNISING FORMATION

By

John Francis Salvino

The diagenetic history of the Munising sandstone is determined by a petrographic examination using thin sections, grain mounts, and SEM. Crosscutting and superposition relationships define a paragenetic sequence; 1) Compaction, which is more severe in the Chapel Rock member, 2) Feldspar and quartz overgrowth, 3) Dolomite cementation 4) Garnet dissolution, 5) Calcite and 6) Mosaic silica cementation.

SEM-Energy Dispersive analyses of garnet yielded composition data useful in constraining the source rocks for sandstones. A comparison with Wright's (1938) compiled garnet compositions shows that granites, and biotite and amphibole schist, are likely rock types present in the Munising provenance

Garnet surface textures found in the Munising are significant for two reasons: 1) The textural relationships with surrounding cements indicate that garnet surface textures are dissolution features. 2) Correlation to laboratory experiments suggest that oxalic acid, a weak Fe and Al chelating organic acid was present in the paleo-pore fluids of the Munising Formation.

ACKNOWLEDGMENTS

Research projects such as this thesis have taught me much more than the facts that are printed on the following pages. I have learned to manage long hours, financial demands, social requirements and even a bit of politics. This is my chance to reference those who instructed me in these finer points.

I would like to thank Ben Schuraytz for taking time from his work to discuss my thesis and teach me the heavy mineral separation, grain mounting, and computer graphics techniques. Thanks also to Jerry Grantham, who generously offered me a part time position that enable me to keep taking class hours. Many thanks to Al, Nadine, Chuck, and especially Tim for "lifting the burden" when it was time to put the thesis aside.

I also greatly appreciate the time that my committee members, Drs. T. A. Vogel and D. F. Sibley contributed to understanding the petrology and petrography of my samples. To my committee chairman, Dr. Michael A. Velbel, I want to document my thanks and appreciation for his hours of reviewing, editing and discussing major and minor points during this project.

I want to extend my warmest thoughts of gratitude to Dana for her unending patience, love, and dedication to my work and education.

TABLE OF CONTENTS

LIST OF FIGURES.....vi

LIST OF TABLES.....ix

INTRODUCTION.....1

BACKGROUND

 Sedimentology and Stratigraphy of the Munising
 Formation.....4

 Munising Formation Correlation.....7

METHODS

 Bedrock Exposures and Sampling.....13

 Analytical Methods18

RESULTS

 Mineralogy.....21

 Detrital.....21

 Detrital Clay in the Munising.....25

 Authigenic.....28

 Primary Pore-Space Reduction and
 Textural Relationships.....37

 Compaction.....37

 Syntaxial Potassium Feldspar Cement.....44

 Clay Cement.....50

 Carbonate Cement.....50

 Quartz Cement.....56

 Mosaic Silica Cement.....57

 Secondary Porosity.....59

 Feldspar Dissolution.....59

Garnet Diagenesis.....	61
Surface Texture Comparison Between Munising Garnets and Previously Studied Garnets.....	66
Wedge Mark Variations.....	69
Compositional Independence.....	75
Garnet Dissolution Features.....	78
Garnet Textural Relationships.....	82
DISCUSSION	
Garnet as a Munising Provenance Indicator.....	94
Paragenetic Sequence in the Munising.....	106
Garnet Diagenesis and Possible Implications to Paleo-Pore Fluid Chemistry.....	113
Laboratory Attempts to Produce Wedge-Mark Textures.....	113
Related Surface Textures on Garnet.....	116
Apatite and Garnet Assemblages.....	116
CONCLUSIONS.....	121
Future Studies.....	123
LIST OF REFERENCES.....	125
APPENDIX 1 Petrographic presence absence chart.....	
	131
APPENDIX 2 Mole percent of garnet end-members for Munising garnet grains.....	
	139

LIST OF FIGURES

- Figure 1. Correlation between Cambrian units in Michigan's Upper Peninsula and Wisconsin..11
- Figure 2. Correlation of Cambrian units in the Great Lakes Region.....12
- Figure 3. Map of Alger County, Michigan, outcrop locations.....17
- Figure 4. QFL diagram of Munising Formation sandstones23
- Figure 5. X-ray diffraction pattern of clay minerals from the sand/shale units at the base of Laughing Whitefish Falls.....27
- Figure 6. Calcite is a minor pore filling cement. This thin section is stained for calcite with alizarin red. (Frame Dimensions: 1.0 mm x 1.5 mm).....30
- Figure 7. Small mosaic silica pore lining cement around quartz overgrowths (Frame Dimensions: 0.40 mm x 0.60 mm).....32
- Figure 8. Petrographic micrograph of phyllosilicate material coating detrital sand grains (Frame Dimensions 0.40 mm x 0.60 mm).....36
- Figure 9. Types of grain boundary contacts in sandstones (Pettijohn and others 1973).....38
- Figure 10. Feldspar fractured after the formation of an authigenic potassium feldspar overgrowth PL (Frame Dimensions 0.40 mm x 0.60 mm)..47
- Figure 11. Euhedral feldspar in carbonate cement (Frame Dimensions: 0.40 mm x 0.60 mm)....48

Figure 12.	Euhedral feldspar overgrowths against quartz overgrowths. XP (Frame Dimensions: 0.40 mm x 0.6 mm).....	49
Figure 13.	Idiotopic-C pore lining dolomite crystals, euhedral or subhedral crystals have crystal face junctions at some boundaries. XP (Frame Dimensions: 1.0 mm x 1.5 mm).....	53
Figure 14.	Poikilotopic; Xenotopic-A dolomite XP (Frame Dimensions: 1.0 mm x 1.5 mm)...	54
Figure 15.	Alizarin stained calcite as a late pore filling cement around garnet. XP (Frame Dimensions: 0.40 mm x 0.6 mm).....	55
Figure 16.	Mosaic which silica has nucleated on dolomite, quartz, and feldspar overgrowths. (Frame Dimensions: 0.40 x 0.60 mm).....	58
Figure 17.	Potassium feldspar dissolution in the Chapel Rock Member. The blue area is epoxy. (Frame Dimensions: 0.40 x 0.60 mm).....	60
Figure 18.	Typical grain mount of the heavy mineral fraction of the Miner's Castle member. (Frame Dimensions: 1.0 mm x 1.5 mm).....	67
Figure 19.	SEM of a garnet on a grain mount. The garnet in the foreground has more wedge mark features than the garnet beneath it. (SEM 350 X).....	71
Figure 20.	A round garnet with wedge marks. (SEM 200 X).....	72
Figure 21.	A single garnet grain that has different wedge shape. (SEM 750 X).....	73
Figure 22.	A fine grain garnet with wedge marks shape variations (SEM 750 X).....	74
Figure 23.	Garnet from which compositional data was gathered. (SEM 100 X).....	79
Figure 24.	Garnet from which compositional data was gathered. (light microscope PL).....	80

Figure 25.	The quartz overgrowths mark the former boundary of the garnet grain. The late silica cement has filled in the enlarged pore space around a garnet grain. PL (Frame Dimensions: 0.40 x 0.60 mm).....	84
Figure 26.	Cross polarized light view of Figure 25 (Frame Dimensions: 0.40 x 0.60 mm).....	85
Figure 27.	Iron oxide indicates the former boundary of the garnet grains in this dolomite cemented sample. (Frame Dimensions: 0.40 mm x 0.60 mm)....	87
Figure 28.	Garnet grains that have imbricate wedge marks show enlarged space within the boundaries of the iron oxide ring. (Frame Dimensions: 0.40 mm x 0.60 mm)....	88
Figure 29.	A SEM of a rock chip showing carbonate cement has formed a cast of the original garnet grain prior to garnet dissolution and the formation of the wedge marks. (200 X).....	91
Figure 30.	A close-up the garnet cement contact showing of Figure 29. (500 X).....	92
Figure 31.	Late calcite pore filling cement has formed within the iron oxide rings. (Frame Dimensions: 0.40 mm x 0.60 mm)....	93
Figure 32.	Munising vs. Pegmatite and Granite Garnet.....	100
Figure 33.	Munising vs. Biotite Schist Garnet.....	101
Figure 34.	Munising vs. Amphibole Schist Garnet....	102
Figure 35.	Munising vs. Basic Igneous Garnet.....	103
Figure 36.	Munising vs. Contact Metasilicate Garnet.....	104
Figure 37.	Muinsing vs. Igneous Garnet.....	105
Figure 38.	Summary of the paragenetic sequence in the Munising Formation.....	108

LIST OF TABLES

Table 1. Petrographic Point Count Data.....21

Table 2. SEM-EDS Composition Data for Mosaic Cement.33

Table 3. Grain Boundary Point Count Data.....41

Table 4. SEM-EDS Compositional Data for
Lake Superior Beach Garnets.....66

Table 5. SEM-EDS Garnet Composition Data for Munising
Formation garnets.....77

Table 6. SEM-EDS Composition Data for a
Single Garnet Grain.....81

INTRODUCTION

The purpose of this study is to use sandstone textural relationships and heavy mineral surface textures to describe the diagenetic history of the Munising Formation, and to constrain the paleo-pore fluid chemistry of these sandstones.

The diagenetic history of the Munising is determined by a petrographic examination of textural relationships between grains and cements. By using crosscutting, superposition, and other textural relationships, this study determines the sequence of events that led to the reduction of porosity in the Cambrian Munising Formation and investigates secondary porosity textures (Schmidt and McDonald, 1979 a and b) found in the Munising.

This study also examines garnet diagenesis in the Munising Formation. By determining the relative order of diagenetic events, including garnet diagenesis, in the Munising paragenetic sequence, this study provides further evidence in the debate regarding the formation of garnet surface textures. Previously, these textures have been interpreted to be the result of either

dissolution (Rahmani, 1973), or overgrowth (Simpson, 1976).

Garnet composition generated in this study is used to suggest rock types that were present in the Munising provenance. This is done by plotting Munising garnet data on garnet composition ternary diagrams compiled by Wright (1938).

Surface textures on garnet have been used to infer certain implications about paleo-pore fluid composition. Laboratory experiments have replicated certain surface textures on natural garnets (e.g. Bramlette, 1929; McMullen, 1959; Gravenor and Leavitt, 1981; Orr and Folk, 1983; Hansley, in press). This study attempts to correlate the petrographic evidence of paleo-pore fluids from these sandstones with the composition of solutions used to produce garnet surface textures in the laboratory.

The study area for this report is within 15 miles of the southern shore of Lake Superior, from the western edge of Alger County to the eastern edge of Chippewa County in the Northern Peninsula of Michigan.

This thesis presents the results of this study in four parts:

(3)

1. The previous work on sedimentology and stratigraphy of the Munising Formation, compiled from the literature;
2. The mineralogy of the Munising, including detrital and authigenic minerals;
3. The diagenetic history of these sands, including reduction of primary porosity and the formation of secondary porosity;
4. The implications of garnet surface textures for the paleo-pore fluid chemistry.

Finally, I summarize the conclusions and present possible avenues of further research.

**SEDIMENTOLOGY AND STRATIGRAPHY OF THE MUNISING
FORMATION**

In 1907, the upper 250 feet of the Lake Superior Sandstones were designated the Munising Formation by Lane and Seaman. Hamblin (1958) divided the formation into three distinct lithologic units. These units are the basal conglomerate, the Chapel Rock member, and the Miner's Castle member. The basal conglomerate of the Munising Formation rests unconformably on the Jacobsville Formation, forming the contact between the Proterozoic and Middle Cambrian (Kalliokoski, 1982). Throughout the Upper Peninsula, the Munising Formation is overlain by thin to medium bedded sandy dolomites and dolomitic sands of the Trempealeau Formation (locally called the Au Train Formation). Hamblin (1958) reports that the three units can be distinguished on the basis of grain size, sorting, composition, sedimentary structures and heavy mineral content.

Basal Conglomerate Member

The basal conglomerate member of the Munising Formation ranges from 2 to 15 feet thick and is thought to pinch out to the south. It is an orthoquartzite, with small amounts of slate, basalt, granite, and sandstone

pebbles. The basal member is thought to have been deposited by a transgressive sea over a low relief surface (Hamblin, 1958). This member is not included in this study because sand size heavy mineral grains do not form a significant portion of the unit.

Chapel Rock Member

The Chapel Rock member is in gradational contact with the basal conglomerate. This member consists of nearly pure, well sorted, medium grain quartz sand. The Chapel Rock member is held together by a matrix of angular quartz fragments that act as a clastic binder (Hamblin, 1958). The Chapel Rock member is a texturally and compositionally mature sandstone; however, some of the Chapel Rock sandstones are poorly sorted, lithic-rich sandstones that are also held together by an angular quartz framework.

The predominant sedimentary structure in this member is the large scale trough crossbedding. Trough sizes range from 3 to 600 feet in width and averages around 30 feet (Hamblin, 1958). Typically, these troughs are on the order of five to ten feet thick. This large scale crossbedding is thought to have been produced in a marine environment (Hamblin, 1958; Haddox 1982). Ripple marks are also present in this member. Mud

cracks are present in the shale bed at the top of the Chapel Rock member. These indicate that the Chapel Rock member was subaerially exposed and suggest that a disconformity exists between the Chapel Rock member and the Miner's Castle member (Hamblin, 1958).

Miner's Castle Member

The Miner's Castle member is a less well indurated sandstone than the Chapel Rock. The contact between these two members usually forms a small terrace along the lake shore as the less resistant Miner's Castle erodes faster than the Chapel Rock. Hamblin's (1958) work shows that the Miner's Castle member is poorly sorted. Grains range in size from clay size to pebble size. Poorly sorted sandstones that contain clay and pebbles are present at the base of the Miner's Castle. Hamblin states that the sandstones become better sorted towards the top of the unit. In the Miner's Castle, well rounded grains are sand size and larger, but the fine sand and silt grains are subrounded to subangular.

Crossbeds in the Miner's Castle member differ from the Chapel Rock member. These crossbedded units are four to six inches thick, rather small compared to the extremely large scale crossbeds of the lower member. Planar bedding units in the Miner's Castle member range

from two to eight inches thick and can be traced for miles laterally (Hamblin, 1958). Mud cracks are also present in the shale units. Other sedimentary structures include ripple marks and concretions.

Munising Formation Correlation

The early studies on the Cambrian sandstones in the Upper Peninsula are described by Hamblin (1958). I will briefly introduce a review of previous stratigraphic work which has provided the foundation for my study. This work shows the problems that arise in correlating the essentially unfossiliferous Cambrian sandstones.

Historically the term Lake Superior Sandstones was first applied to the lowest Paleozoic rocks along the north shore of Northern Michigan in 1814 by Douglass Houghton. Later in 1873 the contact between lower red hard sandstone and upper white sandstone was considered gradational with the upper white friable sandstone. At this time, the Lake Superior Sandstones were correlated with the Potsdam Sandstone in New York. The Lake Superior Sandstone was divided by Lane and Seaman into the Freda Sandstone, the Jacobsville Sandstone, and the Munising Sandstone. The Munising referred to the light sandstone which outcrops as bluffs near Munising,

Michigan. It composes the upper 250 feet of the former Lake Superior Sandstone.

Thwaites considered the Munising Formation correlative with the Dresbach, Mazomanie, and the Trempealeau of Wisconsin. Also at this time, the contact between the Jacobsville and the Munising Formation was considered disconformable. A later interpretation by Cohee (1945) stated that the Munising Formation was equivalent to the Eau Clair, Dresbach and Franconia formations.

Oetking (1951) studied the stratigraphic relationships of the Lower Paleozoic rocks in the Munising area. In his report, Oetking recognized a break in the heavy mineral suites within the Munising Formation and correlated the Munising with the Dresbach and Franconia. Oetking reported no corresponding change in the lithology through the section.

Driscoll (1959) studied the heavy minerals along the North Shore of the Upper Peninsula. He reported that the break in the heavy mineral suite occurred at the contact of the Pictured Rocks [Chapel Rock] member and the Miner's Castle member. According to Driscoll, the Chapel Rock member of the Munising Formation is correlated with the Dresbach whereas the Miner's Castle

member represents a transgressive phase and is correlated with the Franconia of Wisconsin.

Ostrom (1967) composed a geologic cross section from the outcrops at Miner's Castle to Walworth County, Wisconsin. Figure 1 depicts correlations between Michigan and Wisconsin stratigraphic units. He concludes that the Munising Formation of Northern Michigan is correlative with the Wonewoc Sandstone in Wisconsin. He also divides the Wonewoc Sandstone into two members: the lower member, Galesville, correlates with the Chapel Rock member; and the upper member, Ironton, correlates with the Miner's Castle member. These correlations are based on "similarities between stratigraphic position, lithology, mineralogy, and fossil content." (Ostrom, 1967).

Correlations between the members of the Munising Formation and the Cambrian sandstones in the Lower Peninsula are difficult. Figure 2 shows the terms presently used. There are no outcrops of Cambrian sands in the Lower Peninsula so data is limited to core samples and cuttings. Oetking's (1951) correlations with the Cambrian in Wisconsin are based on heavy minerals.

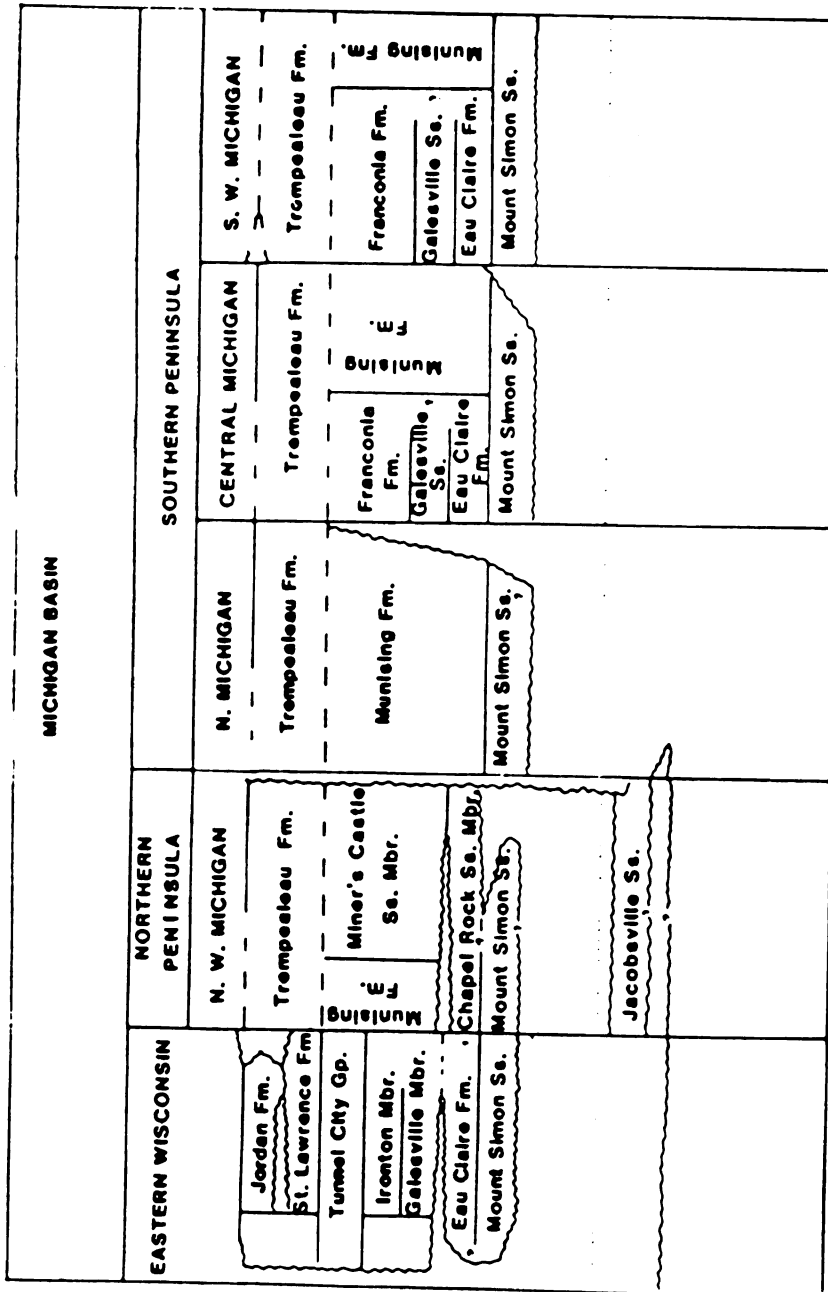
As yet, there have been no widespread heavy mineral studies of Cambrian samples in the Lower Peninsula. Also, there is no fossil evidence from the Cambrian in the Lower Peninsula. However, according to Hamblin's paleogeography during Miner's Castle time the Cambrian seas may have transgressed over the ancient "Northern Michigan Highlands" and into the embryonic Michigan Basin.

As a result, this study is only directly applicable to the outcrops of the Munising Formation in the Northern Peninsula of Michigan and should not be extrapolated any distance into the subsurface.

Figure 1. Correlation between Cambrian units in Michigan's Upper Peninsula and Wisconsin

SOUTHERN WISCONSIN			UPPER PENINSULA	
GROUP	FORMATION	MEMBER	MEMBER	FORMATION
	ST. LAWRENCE	BLACK EARTH		AU TRAIN
TUNNEL CITY	LONE ROCK	RENO	MINER'S CASTLE	MUNISING
	MAZOMANIE			
ELK MOUND	WONEWOC	IRON TON	CHAPEL ROCK	
	EAU CLAIR	GALESVILLE		
	MT. SIMON			
				JACOBSVILLE

Figure 2. Correlation of Cambrian units in the Great Lakes Region (Shaver, 1980)



BEDROCK EXPOSURES AND SAMPLING

The Munising Formation bedrock exposures stretch across the Upper Peninsula in a thin band that is structurally related to the Michigan Basin (Martin, 1957). The principal exposures of the Munising Formation are at the Pictured Rocks National Lakeshore, and at waterfalls located within 15 miles of the southern Lake Superior shore. The Pictured Rocks are vertical cliffs located directly above the lake. These cliffs are between twenty and two hundred feet high and inaccessible except by rope or boat. Most of the interior of the Upper Peninsula is covered by glacial drift and the best bedrock exposures occur at waterfalls. These waterfalls generally expose 50 to 100 feet of the Munising Formation. In this study the waterfalls proved to be the most accessible and easiest outcrops to sample.

The outcrop locations which were used in this study are found on Figure 3 (with the exception of the Tahquahmenon Falls which are located near the border between Chippewa and Luce Counties, Michigan). Principal sampling areas are Laughing Whitefish Falls, Miner's Falls, Chapel Falls, Tannery Falls, and Mosquito Falls as well as the Pleistocene lakeshore

west of Little Beaver Lake. Some samples were also collected at Munising Falls, Wagner Falls, Tahquahmenon Falls, and Hurricane River, and at the type localities for the Munising members: Chapel Rock and Miner's Castle.

Laughing Whitefish Falls (T46N, R22W, sec. 16) exposes almost the complete section of the Miner's Castle member. Samples were collected from exposures along the cliff wall approximately one to ten feet below the crest of the falls and at the base of the falls. Sampling in the stream bed exposure was impossible.

Sampling at Miner's Falls (T47N, R18W, sec. 14) was limited to the stream bed just below the caprock. (This was done to preserve the scenic area maintained by the National Park Service.) At Chapel Falls (T48N, R17W, sec. 28) sampling was also limited to the stream bed and just beneath the crest of the falls.

The exposures at Tannery Falls (T46N, R19W, sec. 1) and at Mosquito Falls (T48N, R17W, sec. 30) are along small cliff walls and next to the stream bed. Sampling at these locations was not restricted.

The Pleistocene lakeshore exposures located east of Little Beaver Lake are ancient shore cliffs composed of

the Chapel Rock member. Samples were taken at various locations from large scale crossbedded outcrops.

Samples were collected from the Miner's Castle member exposure at Wagner Falls. At this location only a resistant silica cemented layer yielded a good sample. In the stream bed of the Hurricane River a large crossbedded unit and a planar bedded unit were sampled. At Lower Tahquahmenon Falls samples were collected from the planar, non-crossbedded units of the Chapel Rock member.

Index to Figure 1

- 1) Laughing Whitefish Falls
 - 2) North of Munising
 - 3) Wagner Falls
 - 4) Tannery Falls
 - 5) Munising Falls
 - 6) Miner's Castle
 - 7) Miner's River & Miner's Falls
 - 8) Mosquito Falls
 - 9) Chapel Falls
 - 10) Chapel Rock
 - 11) Little Beaver Lake
 - 12) Hurricane River
-
- C Chatham
- M Munising
- GM Grand Marais

OUTCROP LOCATIONS ALGER COUNTY

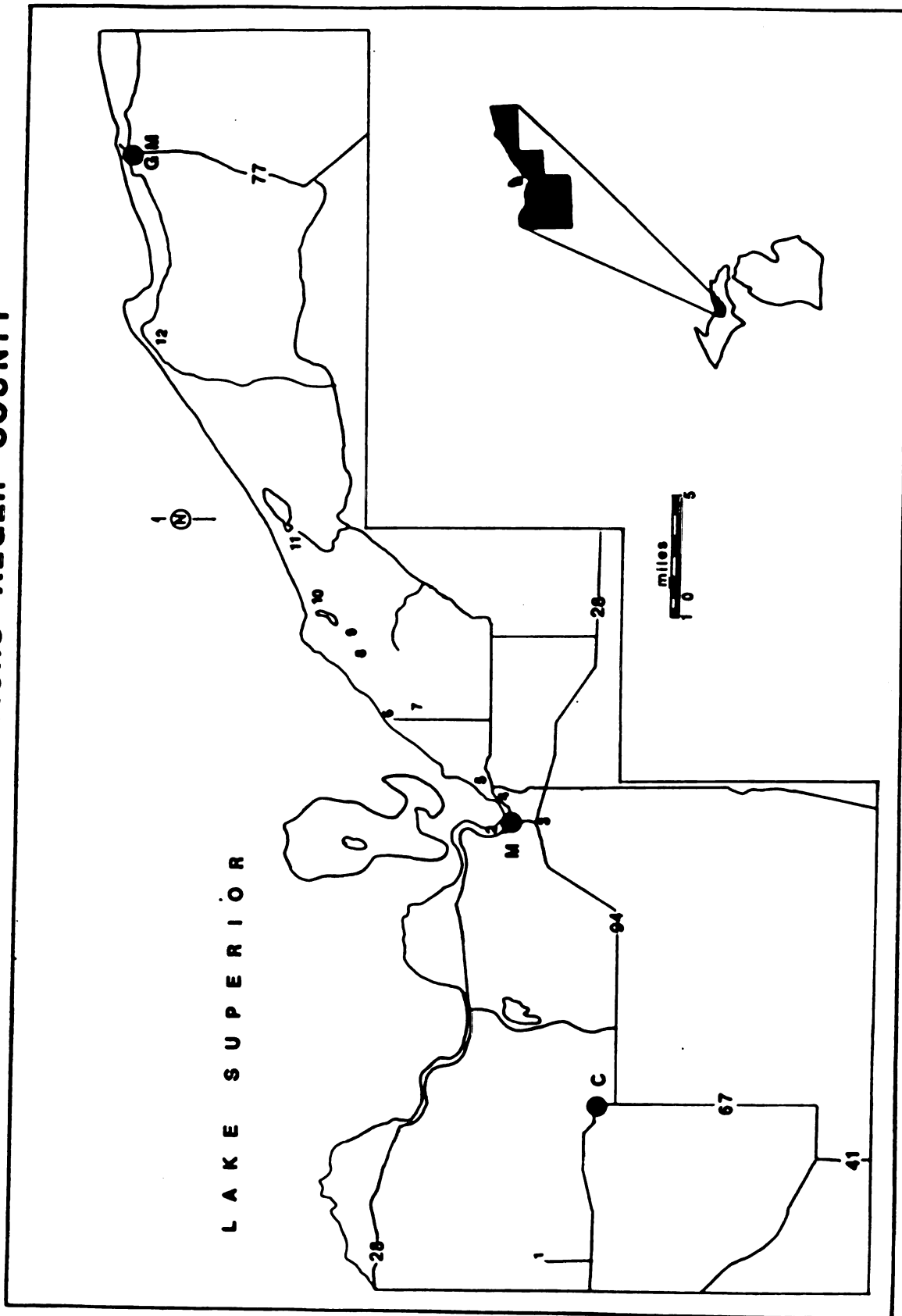


Figure 3.

METHODS

Petrographic Thin Sections

Hand samples were cut into chips, and blue dyed epoxy was vacuum impregnated into the pore space. Each chip was then ground on a coarse grinding wheel at least one grain depth beneath the disturbed surface prior to attaching it to a petrographic slide. Each thin section was ground to 30 microns thickness and coated with immersion oil and a coverslip. Carbonate cemented samples were later cleaned with acetone and stained with alizarin red.

Grain Mounts

Grain mounts were prepared differently depending on the type of cement. The friable uncemented or poorly cemented samples were disaggregated by hand crushing. The dolomite cemented samples were placed in acetic acid for twenty one days. Hard crushing was avoided on these samples in order to preserve the original grain surface textures. Strong acids such as HCl were not used to disaggregate the samples because of their potential 1) to dissolve certain minerals, such as apatite (Nickel, 1973), and 2) to alter the surface textures of the heavy and light minerals. Acetic acid was chosen because it has little effect on the surface

texture of garnet (Hansley, in press). The disaggregated dolomite cemented samples were washed to remove any residual salts from the acetic acid. Quartz cemented samples were lightly crushed with a hammer to avoid fracturing grains. This seemed to give good results; the grains separated along the crystal faces of the quartz overgrowth cement.

The disaggregated samples were separated into light and heavy fractions using bromotetramethane (sp.g. 2.90). The light and heavy fractions were rinsed with acetone to remove bromoform residues. Three types of grain mounts were made from the separates: petrographic mounts, scanning electron microscope (SEM) mounts, and mounts for the scanning electron microscope energy dispersive (SEM-EDS) chemical analysis.

Petrographic mounts were made by embedding the heavy mineral separate into epoxy on a petrographic slide. SEM mounts of heavy minerals were made by placing an adhesive coated brass or aluminum stub on a random portion of the heavy separate. SEM mounts of the light fractions were made simply by spreading a random selection of the grains on the mount. Rock samples were mounted using carbon paint. Approximately one gram of garnet was hand picked for the EDS analysis from the heavy separates of twelve samples. These

garnets were mounted in epoxy, ground and polished. All grain mounts made for either SEM were carbon coated.

X-ray Diffraction Sample Preparations

Petrographic observations allowed me to pick sandstones with a sizeable portion of clay. These sandstones were individually crushed and ground using a ceramic mortar and pestle and stirred in distilled water. The less-than-two micron fraction was separated using Stokes' law for size and settling velocities. The this fraction was concentrated on a Millipore filter (0.45 micron nominal pore size) by vacuum-extracting the water. Untreated samples were then mounted on a glass slide. Prior to mounting, treated samples were saturated with KCl or MgCl solution by passing one to two milliliters of one normal KCl or MgCl through the clay fraction. The samples were glycolated in the same way. Potassium saturated samples were heated to 300 degrees C and 600 degrees C in a furnace.

MINERALOGY**Detrital**

In this section I describe the detrital mineralogy of the two members of the Munising Formation. All of the observations presented below are documented in this study with photomicrographs and tables. Hamblin's (1958) work covered a larger area of the Munising Formation than this report and included core data. For these reasons, Hamblin's work is used to describe overall member mineralogy, and I support his determinations with observations made during this study.

Chapel Rock Member

The detrital portion of both the Chapel Rock and the Miner's Castle members of the Munising Formation is dominantly quartz. The lower member contains mature sandstone beds consisting of 78-98 percent quartz (Figure 4; Table 1). However, there are some sections in the lower member that contain abundant lithic fragments. These fragments are polycrystalline quartz, phyllosilicate, metamorphic fragments (schist-like) and microcrystalline quartz. Lithic rich sands in the Munising contain more potassium feldspar than the quartz arenites. Feldspar in the Chapel Rock ranges

from 0 to 22 percent (Table 1). The most lithic-rich sands were sampled north of Munising on the lakeshore just east of M-28.

The heavy minerals of the Chapel Rock member constitute one half to one weight percent of the sandstone (Hamblin, 1958). Zircon is the most abundant heavy mineral. Brown tourmaline is also present along, with black, blue, and green varieties. Some apatite occurs, along with some rutile (Driscoll, 1959; Hamblin, 1958), in the Munising. Magnetite, hematite, and ilmenite make up the opaques. Garnet is less abundant in the Chapel Rock member than the Miner's Castle member.

Miner's Castle

The Miner's Castle member is composed of 84 to 100 percent quartz (Table 1) with minor amounts of feldspars, and heavy minerals making up one to two percent by weight of the Miner's Castle member. The heavy minerals of the Miner's Castle member form a simple assemblage of garnet, zircon, tourmaline, leucoxene and opaque minerals. Garnet is predominant and usually composes 95 to 100 percent of the heavy mineral fraction of Miner's Castle sands (Hamblin, 1958).

Figure 4. QFL diagram of Munising Formation sandstones

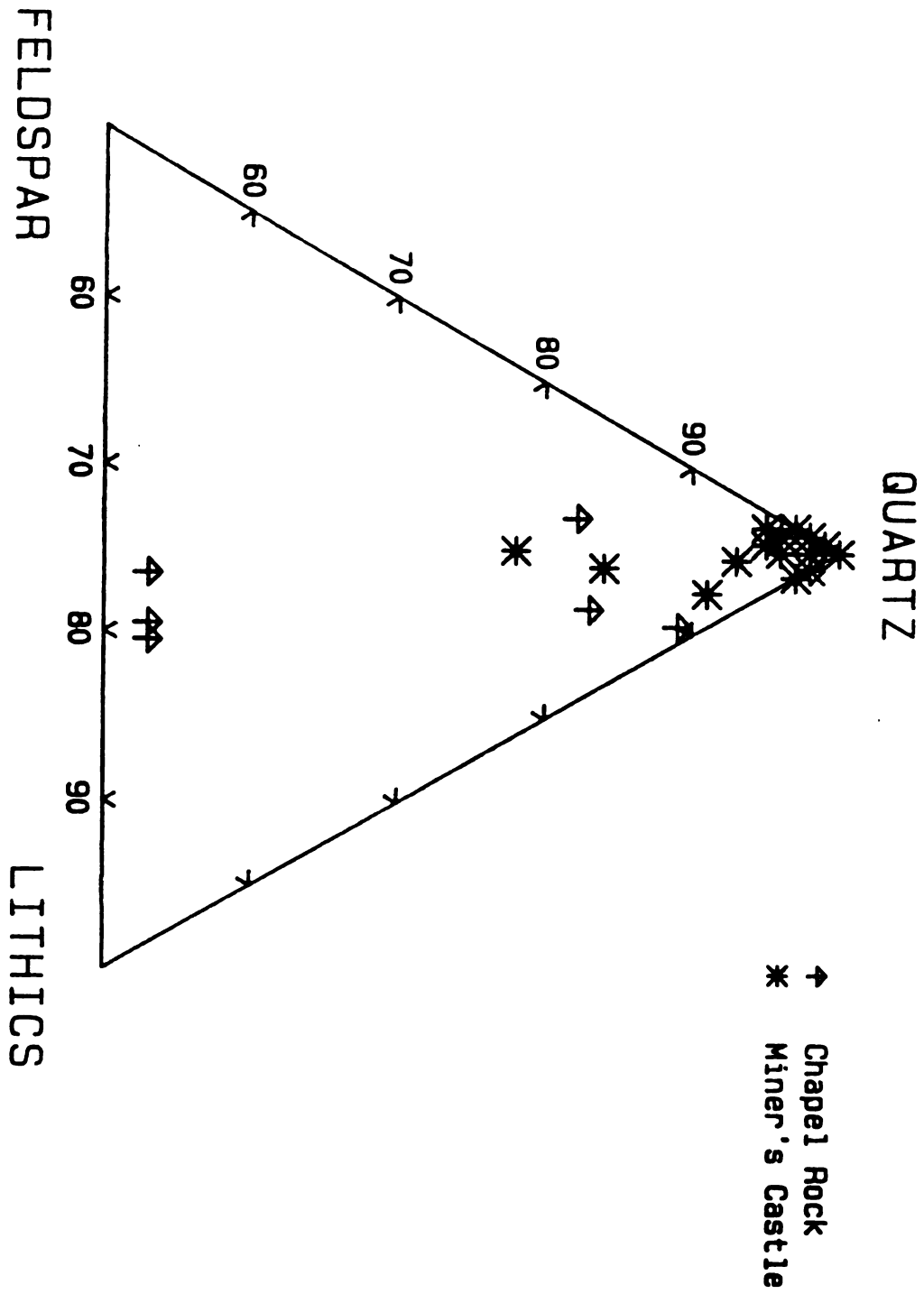


TABLE 1
PETROGRAPHIC POINT COUNT DATA

<u>SAMPLE</u>	<u>FORMATION</u>	<u>QUARTZ</u>	<u>KSPAR</u>	<u>LITHICS</u>
9-21-A	CH	53	18	29
9-21-B	CH	53	19	28
10-26-A	CH	53	22	25
10-26-I	CH	89	1	10
10-27-C	CH	83	11	7
10-27-A	CH	83	5	12
10-23-D	CH	98	0	2
10-25-C	MC	96	3	1
10-25-D	MC	98	0	2
10-25-J	MC	95	4	1
10-25-N	MC	98	2	0
10-25-O	MC	95	3	2
10-25-P	MC	100	0	0
10-25-Q	MC	98	2	0
10-25-S	MC	84	7	9
10-25-R	MC	95	3	2
10-25-A	MC	93	3	4
10-26-E	MC	98	1	1
9-21-E	MC	96	2	2
9-21-F	MC	97	0	3
9-21-G	MC	97	3	0
9-21-H	MC	96	2	2
9-21-I	MC	91	2	7
10-26-N	MC	100	0	0
10-26-M	MC	99	1	0
9-22-E	MC	99	1	0
9-22-F	MC	78	11	11

The only exception to this is the low percentage of garnet at the base of the Miner's Castle in the interbedded sand and shale strata. Driscoll (1959) shows that the garnet percentage varies from about 45 percent at the base of the Miner's Castle to 100 percent at the top.

Detrital Clay in the Munising

The only visible detrital clay in the sandstones of the Munising Formation occurs at the base of the Miner's Castle. Hamblin, (1958) and Bergquist (1920) report thin blue-gray shale beds interbeds with sand at the base of the Miner's Castle. Samples from Laughing Whitefish Falls were collected from the Miner's Castle base and examined using X-ray diffraction for clay identification.

Figure 5 shows the X-ray diffraction patterns for shale from the interbedded sandstones and shales at the base of Laughing Whitefish Falls. Diffraction peaks at approximately 10, 7, 5, 3.3, 3.23 angstroms) indicate the presence of clay minerals, with 10 and 7 angstrom d-spacings, quartz and feldspar. The broad peak beginning at 12 angstroms and extending to about 10 angstroms is evidence of the presence of illite as a discrete mineral and in a random interlayered structure

MUNISING SAND/SHALE

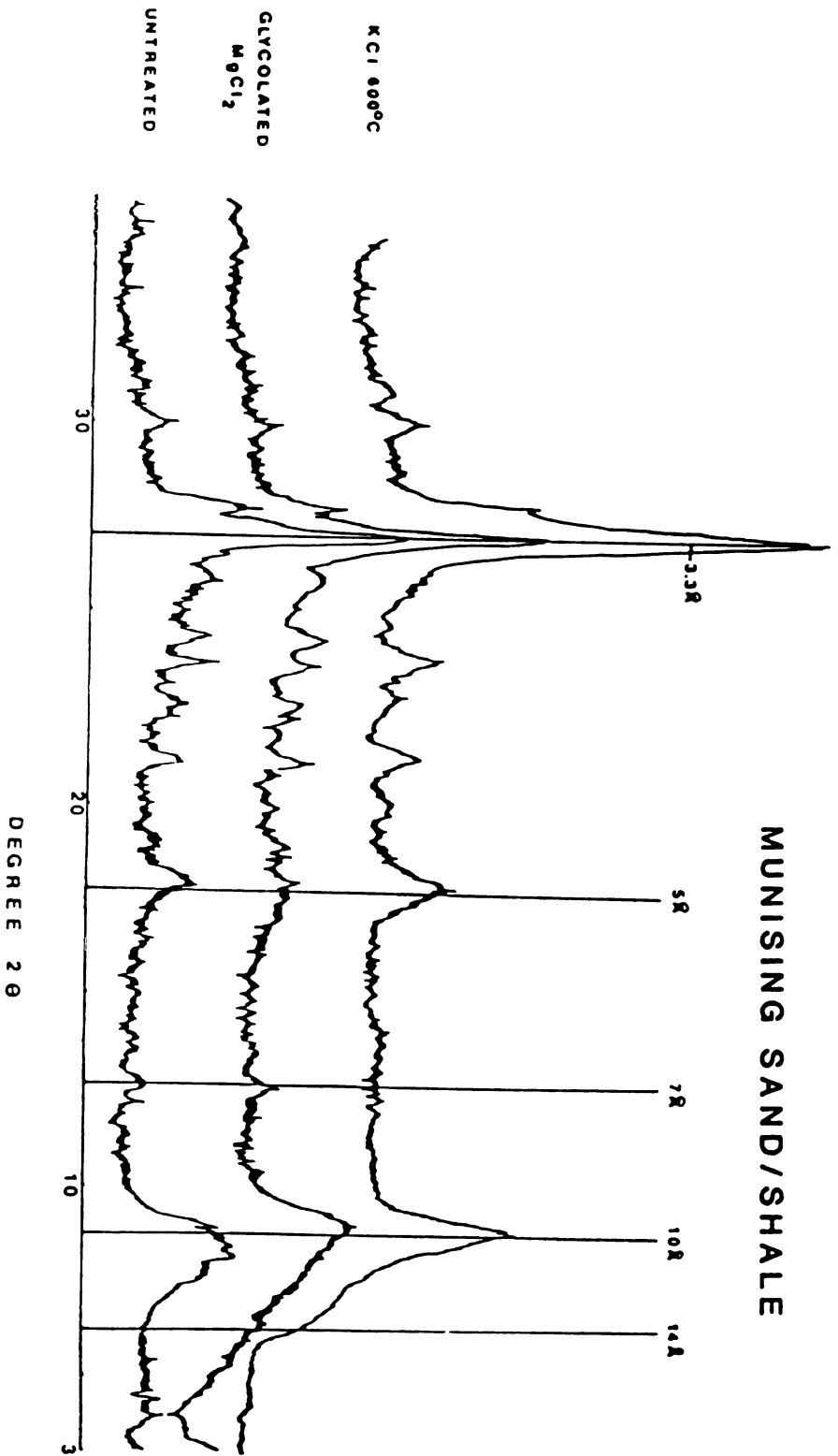


Figure 5. X-ray diffraction pattern of clay minerals from the sand/shale units at the base of Laughing Whitefish Falls

with vermiculite (the peak at 5 angstroms is a second-order peak of this mixture). The consistent peak (one that does not shift with treatment) at about 9.8 angstroms is the evidence of illite in this sample. The potassium chloride saturated sample shows a shift to a 10 angstrom d-spacing indicating the presence of an exchangable clay. The saturated and glycolated magnesium chloride sample shows that none of the clays have expanded to greater than 14 angstroms. This is good evidence that this sample contains a random interlayered illite/vermiculite clay. The heat treated sample lacks the small 7.0 angstrom peak present on the room temperature samples. This is sufficient evidence that some kaolinite is present in this sample. The peaks around 3.3 and 3.2 angstroms are due to quartz (with a third order illite reflection) and potassium feldspar.

Authigenic

This section reviews the authigenic minerals found in the Munising sandstones. These minerals are present in the sandstones as cements and overgrowths on detrital minerals. Their presence in the sandstone is the result of diagenetic events that have taken place after the sandstone was deposited.

I have found authigenic syntaxial overgrowths of feldspar in every thin section that contains detrital feldspar (Appendix 1). Such overgrowths are quite common in Cambrian sands of Wisconsin (Odom, 1975, 1978; Odom et al., 1976). Feldspar overgrowths have also been identified in the Jacobsville Formation (Sibley, 1978) which directly underlies the Munising Formation. Typically, the overgrowths in Cambrian sands are euhedral and grow on detrital microcline or orthoclase feldspar. The Munising examples are also euhedral overgrowths on potassium feldspar cores. Stablein and Dapples (1977) gathered microprobe data on the composition of Cambrian syntaxial feldspar overgrowths. The overgrowths examined are nearly pure end member composition of potassium feldspar. The potassium feldspar overgrowths that Stablein and

Dapples analyzed contained only two percent sodium feldspar.

Both authigenic calcite and dolomite occur as pore filling cements. Dolomite is the dominant carbonate cement, whereas calcite only fills small voids (Figure 6). In outcrop the dolomite-cemented regions occur as lenticular or pod shaped bodies that crosscut the primary sedimentary structures of the sandstone.

Overgrowths of quartz occur on well-rounded quartz grains in certain areas of the Munising Formation. Thin, resistant quartz layers, approximately two inches thick, and not mentioned in Hamblin's work, were found at Laughing Whitefish Falls, Mosquito Falls, Wagner Falls and Miner's Falls. There was no possibility of determining their stratigraphic relationships in the field. However, thin sections show that for each sample the silica cement forms euhedral overgrowths on detrital quartz grains. The overgrowths are in optical continuity with the detrital grain and can be distinguished by a dust ring at the boundary between the cores and the overgrowths.

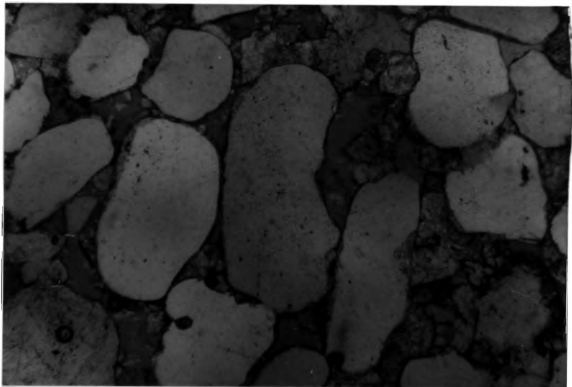


Figure 6. Calcite is a minor pore filling cement.
This thin section is stained for calcite
with alizarin red.
(Frame Dimensions: 1.0 mm x 1.5 mm)

Silica occurs in the Munising Formation not only as syntaxial authigenic overgrowths, but also as mosaic pore lining cement (Figure 7). The crystals are small low (first order grey-white) birefringence, averaging approximately 0.02 mm, subhedral to euhedral. These crystals form interlocking patterns on quartz feldspar and carbonate substrates. This cement is petrographically similar to potassium feldspar cement found in the underlying Jacobsville Formation (Sibley, 1978). Microprobe analyses confirmed that that the Jacobsville cement was truly a feldspar. However, SEM-EDS analysis of the Munising cement indicates that it is a silica cement. Even though the crystals are small and it is difficult to get good analyses the X-ray counts show very little potassium and aluminum relative to silicon (Table 2). This cement differs from a chalcedony cement because the crystals are not fibrous.

The mosaic cement in the Munising lines the pore walls in the quartz cemented sandstones. It has nucleated on quartz overgrowths, dolomite and both detrital and syntaxial potassium feldspar. When the mosaic cement occurs on quartz overgrowths it is not optically continuous with the overgrowth.

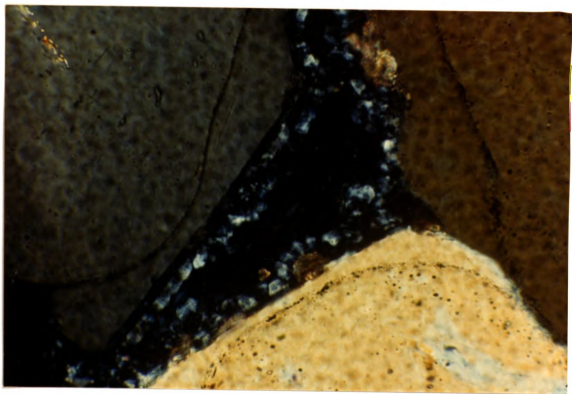


Figure 7. Small mosaic silica pore lining cement
around quartz overgrowths
(Frame Dimensions: 0.40 mm x 0.60 mm)

TABLE 2
SEM-EDS COMPOSITION DATA FOR
FOR MOSAIC SILICA CEMENT

<u>SAMPLE</u>	<u>TEST #</u>	<u>SI</u>	<u>K</u>	<u>AL</u>
10-25-R	1	59275	410	344
	2	69749	-63	565
	3	67122	89	263
	4	70829	195	775
	5	70109	101	713
	6	61845	343	343
10-26-R	1	73791	99	-42
	2	69432	-57	317
	3	58823	51	507

(NOTE; This data represents the number of x-rays counted)

The petrographic examination of the Munising Formation reveals the presence of phyllosilicate material between detrital sand grains. Samples with recognizable phyllosilicate material were from; the Chapel Rock exposures just north of Munising; Tahquahmenon Falls; the Miner's Castle member at Hurricane River, Wagner Falls; and from the sand-shale interbeds at base of the Miner's Castle at Laughing Whitefish Falls (described above).

The minor amount of clay material causes difficulty in identifying authigenic clay in thin section. I ran X-ray diffraction analyses on the less-than-two-micron fraction of the Hurricane River and north of Munising sandstones (I could not obtain a large enough sample from the Wagner or Tahquahmenon Falls samples). The results indicate that quartz and feldspar are present in both samples. Also both samples show randomly interlayered illite/vermiculite. Neither sample contains chlorite or kaolinite.

Authigenic clay may make up a small component of the clay total. Thin section and SEM photographs (Figure 8) indicate that clay material is present as thin pore linings and coatings on detrital quartz

grains in the Wagner, Taquahamenon Falls, and Hurricane River samples.

Wilson and Pittman (1977) state that the most reliable criteria for distinguishing authigenic clay are: (a) delicate morphology; (b) occurrence of the clay as pore linings absent only at grain contacts; and (c) a radical difference in composition from detrital clay material. I was not able to obtain evidence of delicate clay morphology, or distinguish a radical difference in clay composition because the amount of clay material in any sample is extremely minor.

However, textural evidence in Figure 8 is the strongest indication that this clay may be authigenic material. The clay is present as pore linings and appears to be absent at grain contacts.

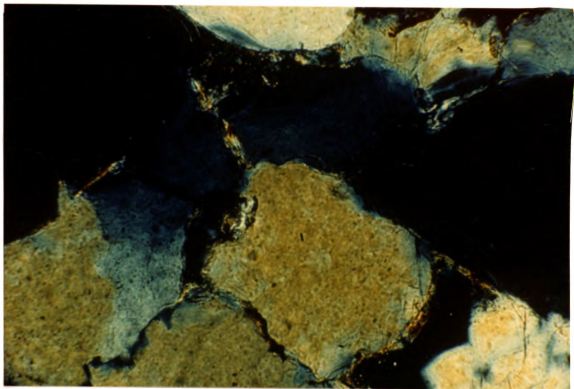


Figure 8. Petrographic micrograph of phyllosilicate material coating detrital sand grains (Frame Dimensions 0.40 mm x 0.60 mm)

PRIMARY POROSITY REDUCTION AND TEXTURAL RELATIONSHIPS

Compaction

Grain orientation and grain fabric are used to determine the amount of compaction that takes place in the Munising sandstones. Pettijohn et al. (1973) and Adams (1964) present results from grain fabric studies that show different fabrics with increasing amount of compaction. These fabrics are identified by the grain to grain contacts. In a two dimensional view, such as a thin section, the contact boundaries may appear as: "floating" grains, in which the contacts are not in the plane of the thin section; point contacts; longitudinal contacts; concavo-convex contacts; or sutured contacts (Figure 9).

Grain reorientation occurs immediately after deposition, if the sands are arranged in a loose framework and not cemented. The majority of the grains touch at single point contacts with nearby grains. As pressure increases, due to continuing deposition, the quartz grains respond by rotating. Grain rotation results in more abundant point contacts and longitudinal contacts (Pettijohn et al. 1973).

(38)

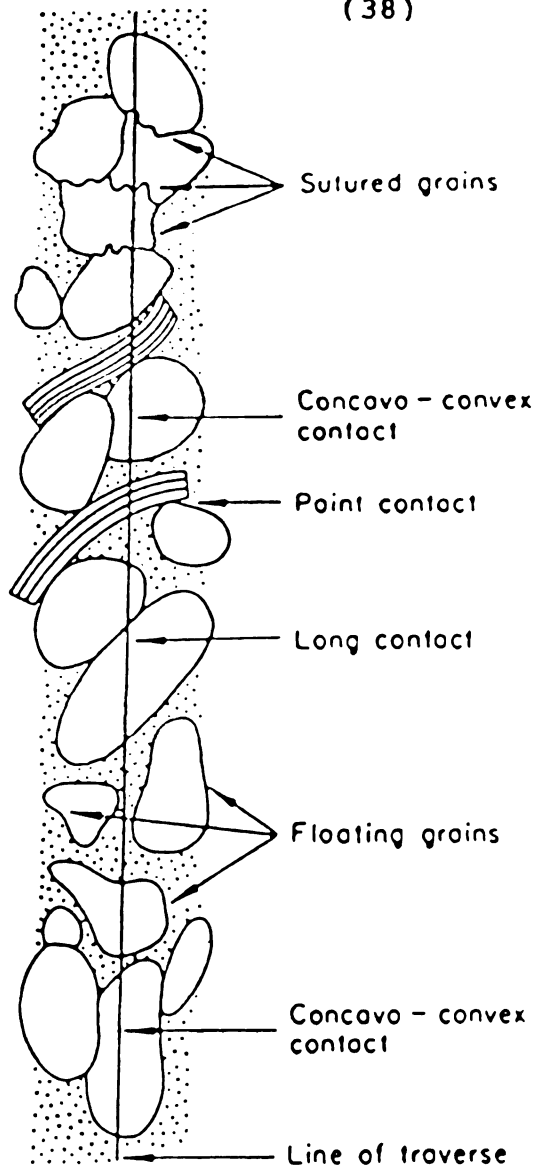


Figure 9. Types of grain boundary contacts in sandstones (Pettijohn and others 1973)



Concavo-convex and sutured (also called crenulated) boundaries indicate that mechanical compaction has initiated quartz pressure solution (Pettijohn and others, 1973; Adams, 1964). Allen (1962, Figure 6) shows that ductile grains are squeezed into nearby pore spaces as the result of compaction.

In the Munising Formation there is evidence that grain rotation and grain deformation have taken place. Petrographic evidence is clear that both members of the Munising Formation have undergone compaction. However, the samples of the Chapel Rock member have undergone a different degree of compaction.

Compaction in the Miner's Castle member was limited to grain rotation. Evidence for this comes from thin section point counts of the grain to grain contacts. The boundary counts were performed by counting the type of boundary intersected on a random traverse across the thin section (after Griffiths, 1958). For example: a point contact was recorded only when the cross hairs fell on a point contact during the traverse; a floating grain was counted when a grain, intersected by the traverse, was not in contact with any grain in the plane of the thin section. This method eliminated

inaccuracy due to grain size differences and bimodal sorting.

The results of these counts are shown in Table 3. Point contacts and floating grains dominate the samples from Miner's Castle sandstones. Long contacts are also present in most of the samples with a wide variation among the different samples. Concavo-convex grain boundaries are also present in a few of the Miner's Castle sands; only in one, 10-25-A, sample are they significant. This sample is distinctly quartz cemented and the grain boundaries may actually be quartz overgrowth boundaries.

The Chapel Rock member has experienced a greater degree of compaction. Thin sections show that the longitudinal contacts compose a greater proportion of the total contacts in the Chapel Rock. There are sutured boundaries in Chapel Rock sandstones. These types of grain fabrics indicate that some degree of pressure solution grains has taken place in the Chapel Rock sandstones. The presence of stylolites in this member (Appendix 1) also indicates pressure solution has taken place.

In the more lithic-rich Chapel Rock samples, phyllosilicate rock fragments have deformed completely

around detrital quartz grains as the result of compaction. The Miner's Castle sandstones do not contain deformed phyllosilicates.

A comparison of the two members was using the "contact" ratio.

$$\text{CONTACT RATIO} = \frac{\text{LONG} + \text{CONCAVO-CONVEX} + \text{SUTURED}}{\text{FLOATING} + \text{POINT}}$$

This ratio, of long contacts plus concavo-convex contacts plus sutured contacts to floating grains plus point contacts, in the Miner's Castle member and the Chapel Rock supports the idea that the lower member was better compacted.

As the contact ratio increase the number of contacts that indicate severe compaction increase. The contact ratio for the Miner's Castle member sandstones are below one with the exception of 10-25-A discussed above and 10-25-J. Dolomite cemented samples have a low contact ratio. The contact ratios in the Chapel Rock member are greater than one. This low contact ratio supports the idea that the lower member experienced more compaction than the upper member.

The amount of average porosity lost due to compaction in the Miner's Castle sandstones is between 10 and 15 percent, assuming an initial porosity of 45 percent. A

(42)

greater amount of porosity loss, average 30 percent to total loss, is evident in Chapel Rock samples, which appears to be entirely due to compaction.

(43)

TABLE 3
BOUNDARY POINT COUNT DATA

CHAPEL ROCK MEMBER						
SAMPLE	FLOAT%	POINT%	LONG%	CC%	SUT%	CONTACT RATIO
9-21-A	0.0	27.5	32.8	24.4	15.3	2.639
9-21-B	0.0	22.7	45.5	19.1	12.7	3.400
10-26-A	0.0	24.4	52.8	17.1	5.7	3.100
10-26-I	0.0	38.5	49.0	9.6	2.9	1.600
10-27-C	0.0	7.5	71.0	18.7	2.8	12.375
9-23-D	0.0	5.6	34.0	16.0	44.4	17.000
10-27-A	0.0	19.6	36.3	31.4	12.7	4.100
10-27-D	0.0	21.0	62.0	15.0	2.0	3.762
10-27-E	0.0	26.7	46.7	17.1	9.5	2.750
MINER'S CASTLE MEMBER						
SAMPLE	FLOAT%	POINT%	LONG%	CC%	SUT%	CONTACT RATIO
9-21-E	16.0	53.0	20.0	8.0	3.0	.449
9 21-F	34.0	48.1	13.2	3.8	.9	.218
9 21-G	45.0	44.0	10.0	1.0	0.0	.124
9-21-H	45.6	40.8	11.7	1.9	0.0	.157
9-21-I	2.9	69.6	25.5	2.0	0.0	.378
9-22-E	1.9	68.6	23.8	5.7	0.0	.419
9-22-F	0.0	52.4	37.3	7.9	2.4	.909
10-25-A	0.0	31.0	40.0	23.0	6.0	2.226
10-25-C	.9	55.0	38.5	5.5	0.0	.787
10-25-D	14.5	63.6	16.4	4.5	.9	.279
10-25-J	0.0	41.9	41.1	15.5	1.6	1.389
10-25-N	9.3	56.1	30.8	3.7	0.0	.529
10-25-O	4.3	66.4	27.6	.9	.9	.415
10-25-P	0.0	82.2	12.1	5.6	0.0	.216
10-25-Q	1.9	64.2	24.5	9.4	0.0	.514
10-25-R	5.5	65.1	23.9	5.5	0.0	.416
10-25-S	0.0	61.2	25.2	10.7	2.9	.635
10-26-E	0.0	50.5	42.7	6.8	0.0	.981
10-26-L	0.0	66.7	27.6	5.7	0.0	.500
10-26-N	21.6	50.0	28.4	0.0	0.0	.397
10-26-M	9.2	61.5	26.6	2.8	0.0	.416

Syntaxial Potassium Feldspar

As discussed above, potassium feldspar overgrowths are found in every sample of the Munising that has detrital potassium feldspar. The amount of pore space lost to the formation of overgrowths is small, ranging from trace amounts to, but not exceeding, approximately one to two percent. The amount of porosity lost in each sample is dependent upon the amount of feldspar in the sample. Odom (1975) and Odom et al. (1976) show that in similar Cambrian sandstones in Wisconsin, the finer grain sandstones have a higher amount of detrital feldspar. This would lead to a greater, but still a relatively minor, amount of porosity loss in these finer sandstones.

Potassium feldspar overgrowths in the Munising Formation formed contemporaneously with and shortly after compaction, and prior to the formation of authigenic overgrowths on detrital quartz grains. They also formed prior to authigenic clay. Evidence for this comes from the textural relationships between the feldspar overgrowths and adjacent authigenic material. This interpretation is based on the assumption that euhedral, authigenic overgrowths form only by unconfined growth into empty space, and not by replacing older material.

Syntaxial potassium feldspar overgrowths formed in the lower member of the Munising prior to complete compaction. Broken detrital potassium feldspars with authigenic overgrowths clearly show that compacting forces continued after the formation of the overgrowths (Figure 10)

In dolomite cemented samples the overgrowths are euhedral adularia bounded by anhedral dolomite (Figure 11). This picture shows that the euhedral potassium feldspar formed prior to the dolomite.

In quartz cemented samples, the euhedral overgrowths on feldspars formed prior to the formation of overgrowths on the quartz (Figure 12). The textures at the boundaries of the authigenic quartz and feldspar in, Figure 12, suggest the following sequence: Initially potassium feldspar grew on detrital potassium feldspar and into the pore space. The feldspar overgrowth continued to grow until it came into contact with a detrital quartz grain. The edge of the feldspar overgrowth in contact with the detrital quartz grain closely follows the boundary of the detrital quartz. The portion of the overgrowth in the pore space shows that unconfined growth yields euhedral boundaries. At some later time, quartz overgrowths formed in the remaining pore space and around the feldspar

overgrowth. The potassium feldspar overgrowth, at least in the case of Figure 12, did not replace the quartz overgrowths.

(47)

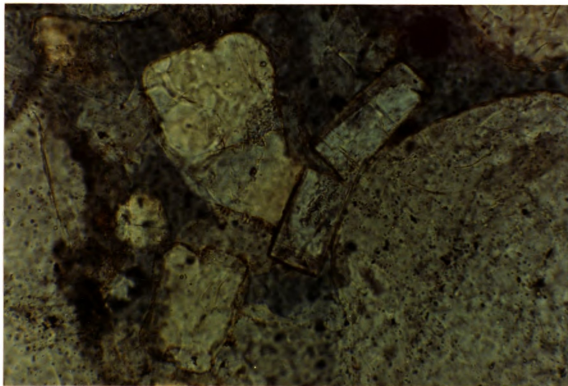


Figure 10. Feldspar fractured after the formation of an authigenic potassium feldspar overgrowth PL (Frame Dimensions 0.40 mm x 0.60 mm)

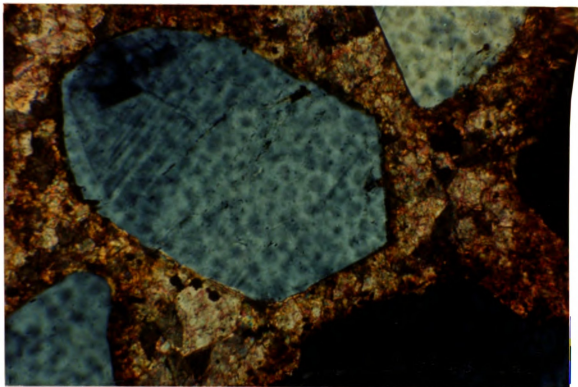


Figure 11. Euhedral feldspar in carbonate cement
(Frame Dimensions: 0.40 mm x 0.60 mm)



Figure 12. Euhedral feldspar overgrowths against quartz overgrowths. XP
(Frame Dimensions: 0.40 mm x 0.6 mm)

Clay

Porosity reduction by clay formation is minor. In a few samples (Appendix 1) there appears to be authigenic clay and potassium feldspar overgrowths. The clay appears to be superimposed upon the overgrowths. (This is again assuming that the potassium feldspar does not replace or displace the clay as the feldspar grows.) Phyllosilicate minerals have grown around the euhedral feldspar overgrowth. The total amount of porosity reduced by the presence of this clay is hard to determine, but in any case it is minor.

Carbonate Material

Carbonate minerals cause the greatest amount of pore space reduction in the Munising sandstones. Dolomite, calcite and siderite are present in these sandstones. Dolomite is the dominant cement in these sandstones. When present, the dolomite cement essentially eliminates the porosity. Calcite cement, in some samples, occurs as a minor pore filling cement in small voids that were not cemented previously by dolomite. Siderite is only present in concretions that occur in layers of the Miner's Castle and the Chapel Rock members.

Both dolomite and calcite occur in the Munising sandstones as pore lining and pore filling cement. The dolomite cement is the dominant cementing material however, it displays a wide variety of crystal textures within these sandstones. The crystal shapes range from euhedral to large anhedral. The crystal sizes vary from small crystals (0.02 mm) which are typically euhedral, to larger crystals (0.15 to 0.7 mm) that are either euhedral or anhedral. Using the dolomite classification system proposed by Gregg and Sibley (1984) I classified the various dolomite textures found in samples of the Munising Formation.

Dolomite present as a pore lining cement, consists of small, euhedral dolomite crystals which nucleated on detrital quartz grains (Figure 13). This is the idiotopic-C dolomite of Gregg and Sibley (1984) Idiotopic dolomite crystals also occur as pore filling cement in these sandstones.

The textural relationships between small euhedral crystals (approximately 0.02 mm) nucleating on the sand grains and euhedral cement in the pores support a single cementation event, even though there are two different crystal sizes. A close examination of the large and small euhedral crystals show that the large crystal nucleation sites are side by side with smaller

crystals nucleation sites, along the detrital grains. All the crystals seem to have nucleated at the same time, but for some reason, only certain crystals grew into the pore spaces between the detrital grains (Pettijohn et al., 1973, Figure 10-6).

Large anhedral crystals of dolomite (averaging approximately 0.7 mm) are also present in the Munising sandstone (Figure 14). These near poikilotopic crystals are present in the well-sorted, compositionally mature sands of the Miner's Castle member. Their tightly packed fabric, curved crystal boundaries, and lack of crystal face junctions place them in the xenotopic-A category of Gregg and Sibley (1984). The coarse, anhedral nature of the cement suggests that the carbonate material grew rapidly from few nucleation sites. The crystals continued to grow until they reached the boundaries of another growing crystal.

Calcite reduces a minor amount of porosity in these sandstones. Calcite is present in dolomite-cemented samples as a late-stage pore filling cement. This cement occurs around garnets and between dolomite rhombs (Figure 15). The calcite is free of dolomite inclusions. The calcite did not replace dolomite; instead it filled only previously uncemented areas.

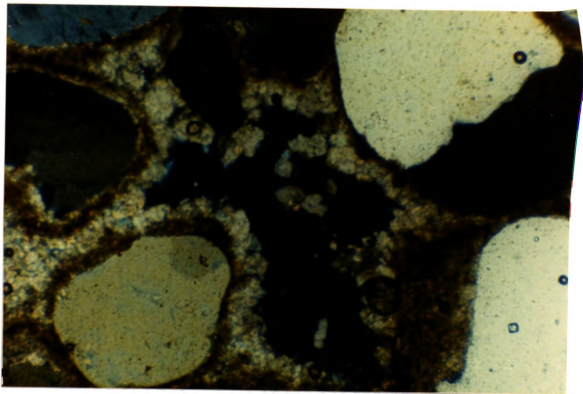


Figure 13. Idiotopic-C pore lining dolomite crystals, euhedral or subhedral crystals have crystal face junctions at some boundaries. XP
(Frame Dimensions: 1.0 mm x 1.5 mm)

(54)

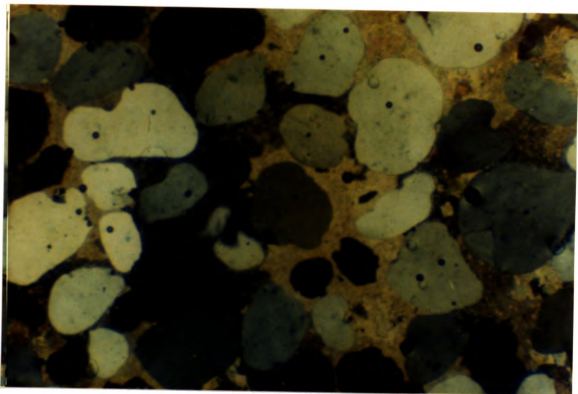


Figure 14. Poikilotopic; Xenotopic-A dolomite
XP (Frame Dimensions: 1.0 mm x 1.5 mm)

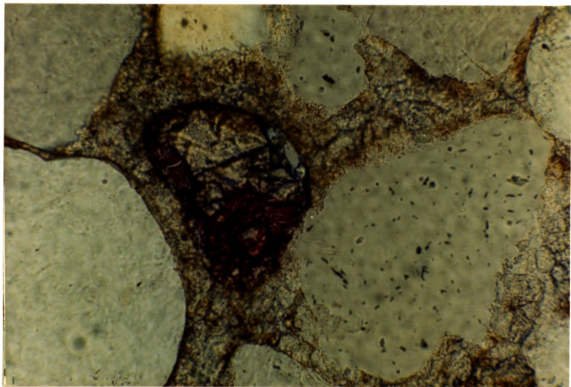


Figure 15. Alizarin stained calcite as a late pore filling cement around garnet. XP
(Frame Dimensions: 0.40 mm x 0.6 mm)

Quartz Cement

Overall, the amount of porosity reduction in the Munising Formation caused by quartz cementation is minor. This is because quartz cemented layers at any one outcrop are apparently few. They do, however, occur at several outcrop locations where at least one small resistant layer is exposed. Where quartz cement occurs, there is only a trace amount of porosity left in the sandstone. Petrographically the quartz overgrowths are large, euhedral and optically continuous crystals, with edges that form equilibrium type boundaries (120 degree angles) with other overgrowths.

The quartz cemented areas adjacent to dolomite cemented layers are typically bounded above and below by dolomite cemented sandstone. Grain boundaries between the dolomite and the quartz show that quartz was present prior to the dolomite crystallization. Quartz overgrowths are euhedral and the surrounding dolomite is anhedral or subhedral.

Mosaic Silica Cement

Mosaic silica cement occurs as a late stage pore lining cement (as discussed in the authigenic mineralogy section). The amount of porosity reduced by this cement is extremely small. The mosaic silica cement appears to have precipitated after the quartz and the dolomite cement. Crystals of this cement are found attached to these minerals and lining pore spaces (Figure 16). The relationship between the silica cement and the quartz overgrowths is clear. The silica pore lining mosaic cement is found growing on the quartz overgrowths but it is not in optical continuity with the quartz overgrowths.

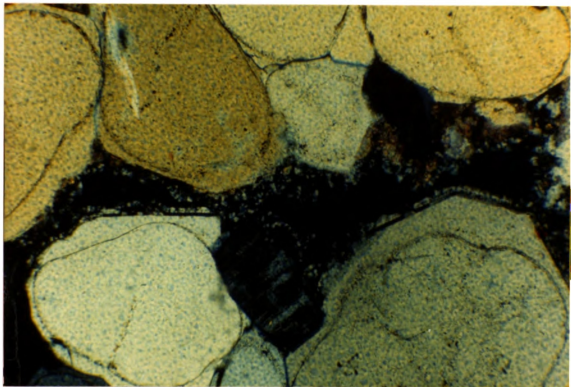


Figure 16. Mosaic which silica has nucleated on dolomite, quartz, and feldspar overgrowths.
(Frame Dimensions: 0.40 x 0.60 mm)

SECONDARY POROSITY

Feldspar Dissolution

Feldspar dissolution textures in the Munising sandstones are similar to those reported by Schmidt and McDonald (1979 b). In thin sections impregnated with blue epoxy, pore spaces are present in the center of a feldspar grain (Figure 17). The center of this grain has dissolved away leaving only the edges of the grain remaining. Evidence of secondary porosity by feldspar dissolution only occurs in samples from the lithic units of the Chapel Rock exposures and from quartz cemented samples from the Miner's Falls exposures. Feldspar alteration in these sandstones does not always lead to secondary porosity. There is evidence that incongruent feldspar dissolution is taking place. Feldspar core and overgrowth alteration occur in other samples as well (Appendix 1) without the removal of the alteration products.

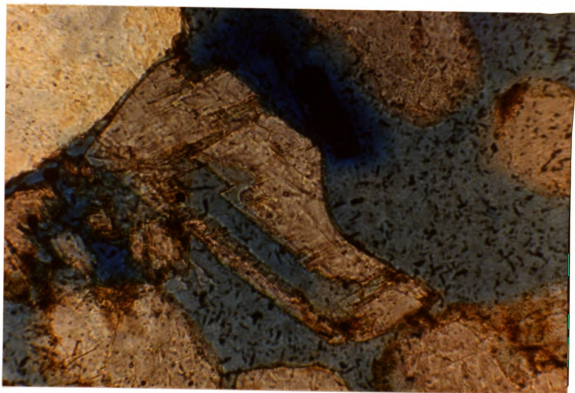


Figure 17. Potassium feldspar dissolution in the Chapel Rock Member. The blue area is epoxy.
(Frame Dimensions: 0.40 x 0.60 mm)

Garnet Diagenesis

In the upper and lower members of the Munising Formation I have identified garnet, zircon, tourmaline, staurolite, and opaque minerals such as iron oxide and ilmenite. This mineral assemblage is similar to the assemblage that Driscoll (1959) and Hamblin (1958) found in the Munising Formation. It differs however in that I have not identified minor amounts of apatite, leucoxene or rutile, as they reported. Garnet is the only mineral that shows any sign of diagenetic alteration.

In the following pages I will present petrographic and SEM observations of the diagenetic alterations of garnet. I will compare the textures on the Munising garnets with surface textures found on garnets in other investigations. I also will show the range of garnet variability in the Munising Formation. Previous workers have argued over whether diagenetic surface textures on garnet are overgrowths or intrastratal dissolution features. I summarize their arguments and present textural data which favor the dissolution hypothesis. These garnet dissolution features are a form of secondary porosity.

Hamblin (1958) reports that garnet varies in abundance in the Munising Formation. The heavy mineral fraction of the lower member contains only one to two percent garnet whereas the upper member contains 90 to 95 percent garnet. My petrographic observations reflect these percentages as well. In general, the Chapel Rock contains only a trace amount (less than one percent) garnet. The Chapel Rock shows no garnet in thin section counts, but it is present in the heavy mineral fraction. This is consistent with the observations made in Hamblin's report. The Miner's Castle garnet content ranges from a trace amount up to five percent of the total number of grains.

Thin sections and grain mounts of the garnets from the Munising Formation reveal diagenetic surface textures. Hamblin (1958) reported "rectangular crystal faces" on the garnet surfaces and stated they were either etch features or overgrowths. The garnet grains have delicate imbricate wedge marks (Rahmani, 1973).

Rahmani's term is used because it does not imply a genetic origin for these features. Wedge marks on garnets are found in every sample (including both the upper and lower members) of the Munising Formation.

The imbricate wedge marks on the Munising Formation garnets are approximately five to ten microns apart.

These marks could not have been formed prior to deposition, because the marks show no signs of abrasion. Garnet is a fragile mineral with a conchoidal fracture and it splinters easily. The delicate wedge-shaped features could not have undergone reworking in the beach and nearshore environment (the suggested paleogeography for this study area Hamblin, 1958) without showing signs of abrasion (Setlow and Karpovich, 1972; Stieglitz and Rothwell, 1978).

A case can be made for the diagenetic origin of garnet surface textures by comparing beach garnets on the North Shore of the Upper Peninsula with Munising garnets. I sampled some of the heavy fraction of black and red sand on the North shore of the Upper Peninsula. This sand is composed of garnet, ilmenite and other heavy minerals that have been deposited on the beach. One must assume that the major source of sand for the beach deposits along the lake are the friable Munising sandstones that form the lakeshore cliffs. My limited sample of beach garnets compositions exhibit (Table 4) a range similar to the Munising garnets. Since wedge marks are present on all the Munising garnets, one would expect to find wedge marks on the beach sands. These black and red sands represent detrital grains exposed to a near-shore, high-energy environment. The

(64)

modern beach grains are fractured and abraded. The beach garnets do not have the wedge marks. From this I concluded that the wedge marks could not survive the high energy environment and could only form under diagenetic conditions

TABLE 4
SEM-EDS COMPOSITION DATA
FOR LAKE SUPERIOR BEACH SAND GARNETS

<u>GARNET</u>	<u>SiO2</u>	<u>Al2O3</u>	<u>MNO</u>	<u>FeO</u>	<u>CR2O3</u>	<u>MGO</u>	<u>CAO</u>	<u>TI02</u>
1	45.77	14.89	0.66	27.05	0.46	9.93	1.24	0
2	47.68	14.56	0.4	25.25	0.46	10.5	0.96	0.25
3	46.54	15.38	0.46	26.75	0.4	9.83	1.26	0
4	46.94	15.24	0.78	25.97	0	9.83	1.26	0

Surface Texture Comparison Between Munising Garnets and Previously Studied Garnet

Garnet features of the Munising Formation match the features of garnet from other sedimentary units.

Hamblin (1958) first reported surface features that resembled crystal faces in the Munising Formation and presented a light micrograph of the garnets. My investigation shows that the garnets of the Munising have imbricate wedge marks like those Rahmani (1973) describes (Figure 18).

Rahmani (1973), Hemingway and Tamar-Agha (1979) Gravenor and Leavitt (1981), Morton (1984), Borg (1986), and Hansley (in press) show SEM pictures of garnets that have imbricate wedge marks. Their pictures are identical to the SEM photographs of garnets in the Munising Formation.

Previous work has shown that wedge marks on garnet are present in sandstones of varied composition and age. Wedge marks on garnet have been found in Upper Cretaceous - Paleocene sandstones of Alberta (Rahmani, 1973), Paleocene quartz sandstones in the North Sea (Morton, 1979 a, 1979 b, and 1984), Upper Triassic arenites in southern Germany (Borg, 1986), and fluvial lithic arenites of the Jurassic Morrison Formation in Northwestern New Mexico (Hansley, in press).

(67)

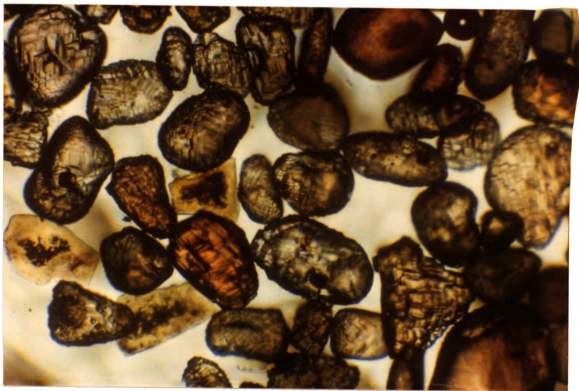


Figure 18. Typical grain mount of the heavy mineral fraction of the Miner's Castle member.
(Frame Dimensions: 1.0 mm x 1.5 mm)

Garnet textures in the Munising differ from the chattermark features reported by Folk (1975), Gravenor and McIelwain (1978) and Orr and Folk (1983). These chattermarks features are microfractures on the surface of a garnet grain that may be enhanced internal fractures. The Pleistocene garnets with chattermarks studied by Orr and Folk (1983) were more prevalent in glacial deposits closer to the soil zone.

The garnet textures in the Munising Formation differ from surface textures on garnet found in the soil zone and in saprolite (Velbel, 1984). Soil zone garnets show randomly distributed etch pits that may be controlled by crystal defects or by inclusions. The etch pits have a six sided, roughly hexagonal shape. These pits indicate a relationship with the internal crystal structure of the garnet in that the orientation of the etch pits walls are parallel. The surfaces of garnets in weathered metamorphic saprolite, beneath the soil zone, do not show etch pits; rather, they have smooth surfaces that are covered with a gibbsite-goethite layer. Velbel concluded that the etch pits in soil garnets were related to organic compounds found in the soil zone, because no etch pits are found on garnets below the soil zone.

Wedge Mark Variations

Within a single sandstone sample heavy fraction the number of garnet wedge marks vary on individual grains. Figure 19 shows a garnet in the center of the scanning electron micrograph that appears to have many wedge marks; so many that the shape of the grain appears to have become more angular. The garnet that is just beneath the center garnet seems to have fewer wedge marks and still maintains a rounded shape. The garnet in Figure 20 also maintains a rounded shape.

Hemingway and Tamar-Agha (1975) suggested that there is a progression from garnets with few wedge marks to garnets that have many wedge marks on the entire surface. They present diagrams showing different stages of the wedge mark formation. Figure 21 shows a garnet grain that exhibits all the various stages that Hemingway and Tamar-Agha discuss. Also the garnet in Figure 22 has wedge marks that are shaped slightly different from the others garnets. This variety of wedge mark shapes are present in heavy mineral fractions of individual samples.

The severity of garnet etching does not appear to be related to the type of cement. One might assume that if grains were sealed in a quartz or carbonate cement they would experience a lesser degree of etching than those in uncemented sandstones. This does not appear to be the case.

The petrographic microscope shows garnets that appear to lack the wedge mark features however the SEM observations show that all garnets observed have some degree of wedge mark formation which is beyond the resolving power of the light microscope.

(71)

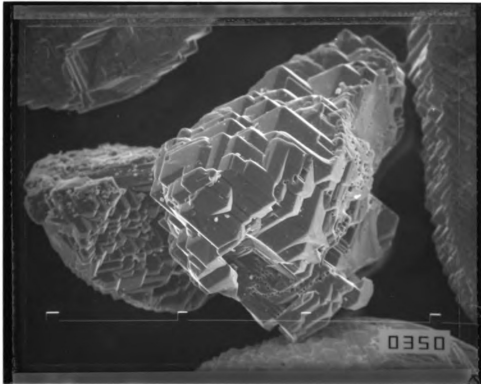


Figure 19. SEM of a garnet on a grain mount. The garnet in the foreground has more wedge mark features than the garnet beneath it. (SEM 350 X)

(72)

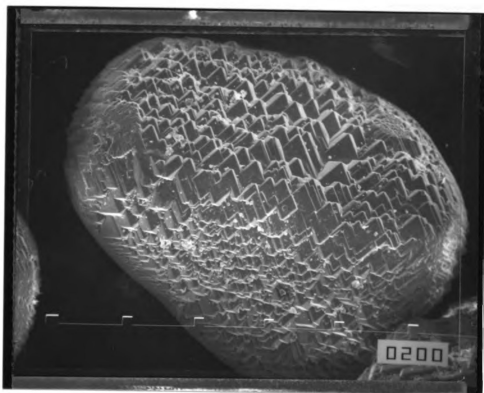


Figure 20. A round garnet with wedge marks.
(SEM 200 X)

(73)

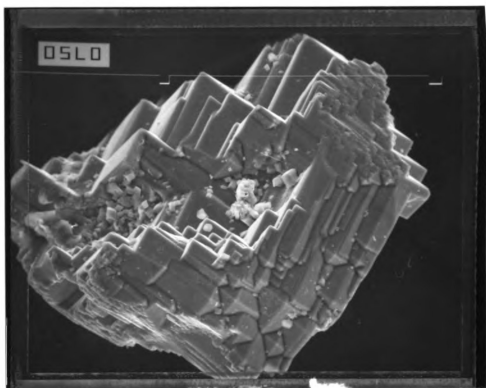


Figure 21. A single garnet grain that has different wedge shape. (SEM 750 X)

(74)

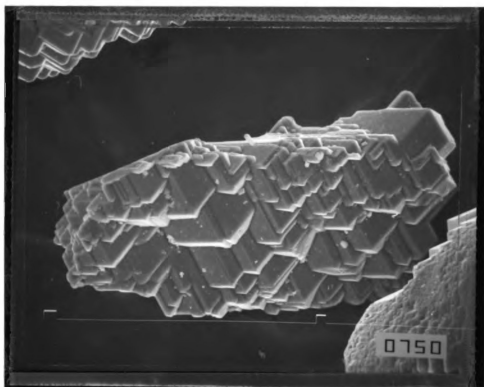


Figure 22. A fine grain garnet with wedge marks
shape variations
(SEM 750 X)

Compositional Independence

The distribution of garnet wedge marks may be independent of composition. Using the SEM-EDS, I obtained the compositions of garnet grains in various samples from the Munising Formation (Table 5). The garnets in the Munising Formation do indeed show compositional variations. Even though I could not identify the surface textures on all the samples and make a direct composition/wedge mark correlation, I concluded that the presence of wedge marks was independent of composition because wedge marks occur on all garnet grains. Gravenor and Leavitt (1981) observed similar chemical variability in garnet composition for naturally etched garnets.

McMullen (1959) found the composition of wedge marked garnets from the Cardium Formation, Alberta was over 81% Mn-rich garnet (spessartine). In my analysis only four garnet grains had a large percentage of Mn and no garnet grain approached 81% spessartine (Appendix 2). Garnet composition within a formation is due to a source area of a single type of garnet. The fact that McMullen found etched spessartine garnets supports the conclusion that etching on garnets is seems to be independent of composition.

TABLE 5
SEM-EDS COMPOSITION DATA
FOR MUNISING FORMATION GARNETS

SAMPLE	RUN	SiO2	Al2O3	MNO	FeO	CR2O3	MGO	CAO	TiO2
10-25-N	1	44.66	17.08	0.55	28.91	0	7.96	0.84	0
10-25-N	2	43.83	16.50	1.31	30.02	0	7.15	1.19	0
10-25-N	3	42.77	16.66	1.57	31.35	0	4.89	2.76	0
10-25-N	4	41.27	16.03	1.46	29.14	0	9.40	2.69	0
10-25-N	5	43.56	18.22	0.91	28.49	0	6.73	2.09	0
10-25-N	6	44.65	15.52	1.09	28.57	0.28	8.70	1.20	0
10-25-C	1	44.03	17.55	0.78	30.69	0	6.02	0.94	0
10-25-C	2	45.90	15.78	17.11	21.21	0	0	0	0
10-25-C	3	44.66	17.57	0.39	26.23	0.66	8.89	1.34	0.25
10-25-C	4	42.52	16.32	19.05	21.51	0	0	0.60	0
9-21-C	1	43.86	18.27	0.64	27.95	0	8.38	0.91	0
9-21-C	2	43.68	16.68	0.67	30.76	0.46	6.46	1.74	0
9-21-C	3	44.51	17.56	0.56	27.29	0	8.56	1.52	0
9-21-C	4	44.74	16.79	0.95	26.87	0.27	8.35	2.02	0
9-21-C	5	43.25	16.47	1.09	29.54	0	3.82	5.83	0
10-25-Q	1	44.55	15.92	0.70	27.76	0	9.00	2.07	0
10-25-Q	2	45.96	15.31	0.51	27.39	0	9.96	0.88	0
10-25-Q	3	47.81	14.68	0.62	26.49	0	9.10	1.30	0
10-25-Q	4	45.64	15.28	0.38	26.65	0.58	0.64	1.83	0
10-25-Q	5	46.78	14.43	0	27.67	0	10.22	0.90	0
10-25-S	1	33.91	14.82	22.26	23.10	0	0	0.68	0
10-25-S	2	50.19	29.11	0	15.04	0	44.44	0.50	0.72
10-26-E	1	44.65	14.56	1.06	30.57	0	7.59	1.57	0
10-26-E	2	46.86	14.81	0.38	24.98	0	11.35	1.62	0
10-26-E	3	44.32	14.20	3.44	34.09	0	2.84	1.11	0
9-21-H	1	44.33	15.00	0.60	29.98	0	8.36	1.35	0.37
9-21-H	2	46.12	14.18	0.55	27.08	0.50	0.79	1.78	0
9-21-H	3	46.17	16.71	1.05	28.73	0	6.54	0.81	0
9-21-H	4	45.85	14.41	0.91	29.98	0	0	8.14	0.71
10-26-L	1	45.04	13.41	1.11	32.19	0	7.34	0.90	0
10-26-L	2	44.68	13.72	0	28.57	0.38	10.68	1.48	0.49
10-26-L	3	43.99	14.89	0.75	29.89	0	8.42	2.08	0
10-26-L	4	44.18	15.08	0	30.33	0	8.30	2.11	0
10-25-R	1	48.07	13.31	0.87	25.91	0.33	10.31	1.20	0
10-25-R	2	45.54	15.76	0.42	30.93	0	6.61	0.75	0
10-25-R	3	46.31	14.77	0.83	26.75	0	10.07	1.27	0
10-25-R	4	44.75	13.99	1.27	33.02	0	5.99	0.97	0
10-25-R	5	48.28	13.24	0.65	24.05	0	12.32	1.45	0
9-21-G	1	45.77	14.89	0.66	27.05	0.46	9.93	1.24	0
9-21-G	2	47.68	14.56	0.40	25.25	0.40	10.50	0.96	0.25
9-21-G	3	46.54	15.38	0.46	26.75	0	9.81	1.05	0
9-21-G	4	46.91	15.24	0.78	25.97	0	9.83	1.26	0
9-21-G	5	47.43	14.60	0.85	24.30	0	5.47	7.34	0

TABLE 5 CONTINUED
SEM-EDS COMPOSITION DATA
FOR MUNISING FORMATION GARNETS

SAMPLE	RUN	SiO ₂	Al ₂ O ₃	MnO	FeO	Cr ₂ O ₃	MgO	CaO	TiO ₂
10-26-M	1	46.49	14.88	1.32	29.45	0	5.62	1.89	0.34
10-26-M	2	48.09	14.11	0.87	27.16	0	8.26	1.50	0
10-26-M	3	46.94	14.43	0.89	22.60	0	10.66	2.50	1.97
10-26-M	4	45.27	14.86	0.88	30.81	0.32	6.78	1.08	0
10-26-I	1	45.78	16.05	0.65	25.24	0	9.29	2.61	0.38
10-26-I	2	49.45	24.79	0	4.15	0	14.77	5.45	1.39
10-26-I	3	49.30	30.55	0.37	16.59	0	1.46	0.65	1.58
10-26-I	4	44.21	16.62	0.74	27.94	0.65	7.49	2.34	0
10-27-A	1	45.50	14.59	0.80	27.29	0.45	9.81	1.57	0
10-27-A	2	49.64	27.53	0	13.22	0	6.42	1.82	1.37
10-27-A	3	57.52	24.92	0	11.86	0.46	4.08	1.16	0
9-21-B	1	47.96	13.91	0	26.33	0	9.63	2.17	0
9-21-B	2	44.55	14.91	0.37	33.33	0	5.74	1.10	0
9-21-B	3	45.76	13.63	0.66	32.34	0	6.34	1.27	0

Garnet Dissolution Features

In the past there has been a controversy over the origin of wedge marks on garnets. Simpson (1976) believes that they are the result of garnet overgrowth on detrital garnets. Other workers believe that the features represent dissolution features.

Gravenor and Leavitt (1981) show that the composition of individual grains of garnet was homogenous. They tested Simpson's (1976) interpretation that the features are overgrowths. Gravenor and Leavitt (1981) address the problem: If the features were actually overgrowths rather than dissolution features the wedges would have a different composition than the center of the garnets. Gravenor and Leavitt (1981) conclude that the garnet wedge marks are not overgrowths. Borg (1986) shows similar evidence of a homogenous individual garnet grain composition in sandstones from Triassic sandstones in Germany. In this study, I have found that a garnet grain that has wedge marks (Figure 23 & 24) is chemically homogeneous (Table 6) from the edge of the grain to the center of the grain.

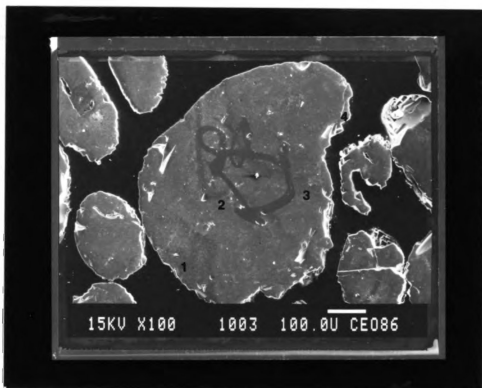


Figure 23. Garnet from which compositional data was gathered. (SEM 100 X)

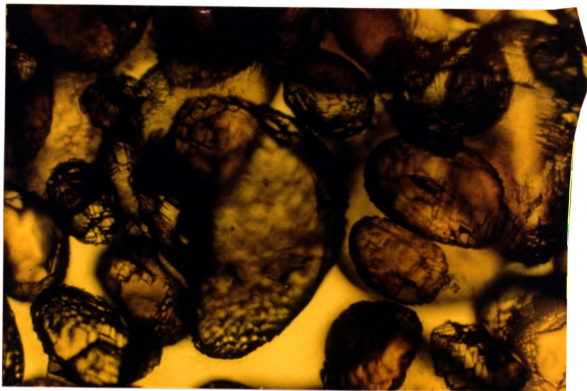


Figure 24. Garnet from which compositional data was gathered. (light microscope PL)

TABLE 6
SEM-EDS COMPOSITION DATA
FOR A WEDGE MARKED GARNET

<u>GARNET</u>	<u>SiO2</u>	<u>Al2O3</u>	<u>MNO</u>	<u>FeO</u>	<u>CR2O3</u>	<u>MGO</u>	<u>CAO</u>	<u>TI02</u>
1	45.77	14.89	0.66	27.05	0.46	9.93	1.24	0
2	47.68	14.56	0.40	25.25	0.40	10.5	0.96	0.25
3	46.54	15.38	0.46	26.75	0	9.81	1.05	0
4	46.91	15.24	0.78	25.97	0	9.83	1.26	0

After performing the experiment I found that it was extremely difficult to be positive that I was indeed analysing the wedge marks. The SEM image presents only the polished surface of the grain and shapes. What appear to be very small (less than ten micron) wedge marks may be only splintered or fractured edges that are artifacts due to sample preparation or the orientation of the grain in the mount. I think that it would be extremely fortuitous to get good composition data from the wedge mark features. Gravenor and Leavitt (1981) took microprobe compositions from twenty or more different locations on single garnet grains. Their large number of observations gave them a better chance to obtain data from a single wedge mark.

Garnet Textural Relationships

Because of the difficulty in obtaining wedge mark composition data, textural evidence between garnet grains, sandstone grains and cement is a better way of showing that the the wedge marks are actually dissolution features. Grain mounts do not show textural; relationships therefore, thin section data must be used. Even in thin sections it is difficult to determine whether these small wedge marks on garnets are present in enlarged pore spaces unless there is a

diagenetic indicator of the former boundary of the garnet grain. One cannot simply assume that the garnet boundary was originally round. Garnet grains are not always round because they fracture easily. The best former boundary indicator is authigenic material that has formed prior to the development of the wedge marks on the garnet surface. An authigenic material present after the formation of the wedge mark also aids in identifying an enlarged space.

Wedge marked garnets in quartz cemented sands occur in enlarged pore spaces. In quartz cemented sands the boundary indicator is the quartz overgrowths. In Figures 25 & 26 the enlarged pore spaces are preserved by in filling, late stage, mosaic silica cement. As presented earlier in the authigenic mineralogy section, mosaic silica cement is a pore lining and pore filling cement that is present on feldspar and quartz overgrowths. Figures 25 & 26 show it is also present around garnet grains.

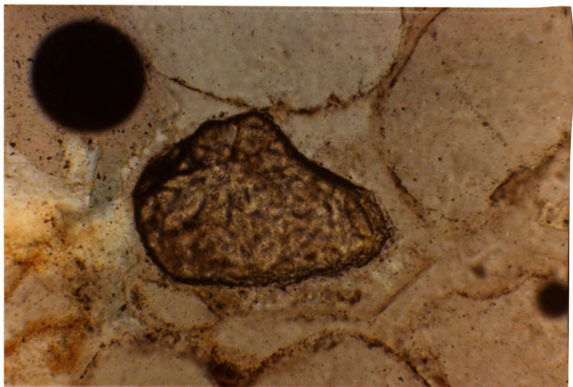


Figure 25. The quartz overgrowths mark the former boundary of the garnet grain. The late silica cement has filled in the enlarged pore space around a garnet grain. PL (Frame Dimensions: 0.40 x 0.60 mm)

(85)

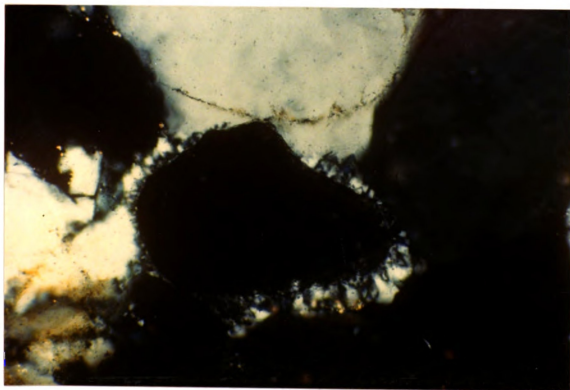


Figure 26. Cross polarized light view of Figure 25
(Frame Dimensions: 0.40 x 0.60 mm)

Quartz overgrowths in this sample grew until they reached the detrital grain boundary of other grains or until they reached the boundary of another overgrowth. The overgrowths grew up to the boundary of the garnet grains. After this occurred, the garnet grain dissolved and formed an enlarged space. The last event in this sequence occurred when the mosaic silica filled in the enlarged pore space.

Garnets with imbricate wedge marks in the dolomite cemented samples are associated with enlarged pore spaces. Again, in many cases the enlarged space is difficult to determine because it is too small. There needs to be an indicator of the garnet's original shape. Small blebs of iron oxide that occur between the garnet grain and the carbonate material give an indication of original grain shape. The iron oxide formed in the carbonate cement of the sample from which Figure 27 was taken. In this sample carbonate cement surrounds all of the sandstone grains and I assumed surrounded garnet grains as well. Enlarged pore spaces have developed around garnet grains as the garnet receded away from the boundary with the dolomite cement (Figure 27 & 28).

(87)

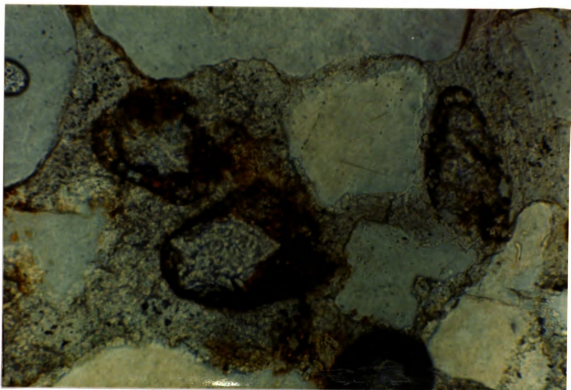


Figure 27. Iron oxide indicates the former boundary of the garnet grains in this dolomite cemented sample.
(Frame Dimensions: 0.40 mm x 0.60 mm)

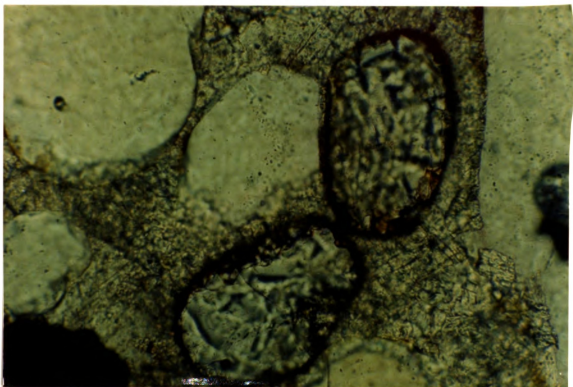


Figure 28. Garnet grains that have imbricate wedge marks show enlarged space within the boundaries of the iron oxide ring.
(Frame Dimensions: 0.40 mm x 0.60 mm)

Since dolomite growth stops at the iron oxide boundary and does not fill in between the wedge marks, the iron oxide indicates the period of time after cementation and prior to garnet dissolution and also gives some idea of the garnet's shape prior to dissolution. The SEM shows this feature quite well. A garnet in a dolomite cemented sandstone is associated with a small space between the garnet and the dolomite that does not contain any cement (Figures 29 & 30); there is a "shell" of dolomite surrounding the garnet. This feature does not exist on quartz grains that do not seem to have undergone dissolution. I believe that this "shell" is a cast of the former garnet grain prior to dissolution.

Around some garnet grains calcite cement has precipitated as a late pore filling cement (Figure 31) within the boundaries of the iron blebs. The garnet in Figure 31 also shows slight wedge marks on the edges. These observations suggest that garnet dissolution took place after the initial cementation event and prior to the calcite pore filling event. Enlarged pore spaces formed as a result of garnet dissolution.

Previous workers also concluded that diagenesis in the sedimentary or near surface environment can cause garnet surface alteration and form wedge marks and

dissolution pits on the surface of garnet grains (Bramlette, 1929; Rahmani, 1973; Simpson, 1976; Gravenor and Leavitt, 1981; Orr and Folk 1983, Velbel, 1984; Borg, 1986; Hansley, in press).

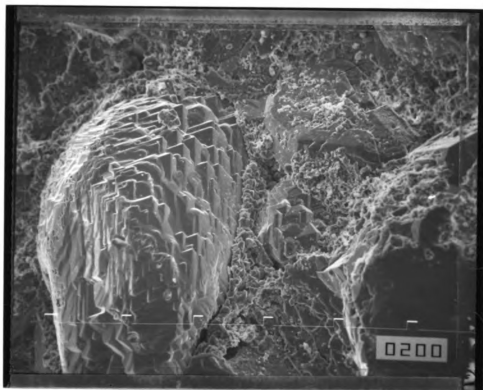


Figure 29. A SEM of a rock chip showing carbonate cement has formed a cast of the original garnet grain prior to garnet dissolution and the formation of the wedge marks.
(200 X)

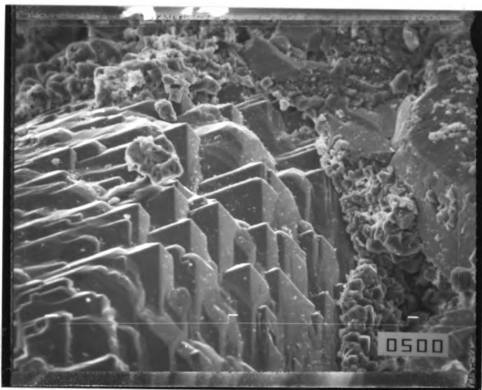


Figure 30. A close-up the garnet cement contact showing of Figure 29. (500 X)

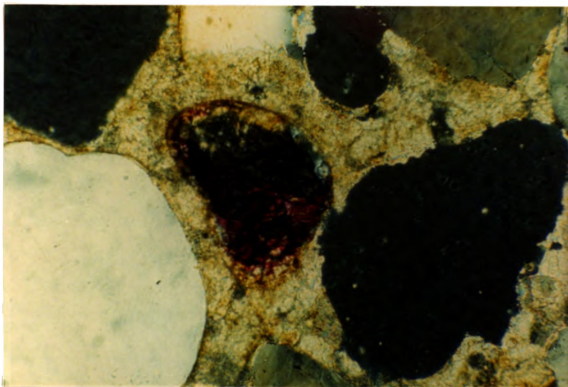


Figure 31. Late calcite pore filling cement has formed within the iron oxide rings.
(Frame Dimensions: 0.40 mm x 0.60 mm)

GARNET AS A PROVENANCE INDICATOR

The SEM-EDS has provided data that can be used to interpret the provenance of the Munising Formation. An abundance of accurate quantitative heavy mineral composition data from a sandstone unit is a useful tool in determining the primary source area of the sandstone. After a brief discussion on the use of composition data from heavy minerals as provenance indicator, I present how I used garnet compositions to constrain the primary source rock types for the Munising Formation. I will also discuss some of the potential limitations to using garnet data and how the true provenance of the a sandstone may be obscured.

Using the SEM-EDS is a simple method to obtain composition data from detrital sand grains. Feldspar (Travena and Nash, 1981 and Maynard, 1984) and clinopyroxene (Cawood, 1983) microprobe data have been used to indicate provenance. Morton (1986) used garnet compositions to constrain the source terrain of the Triassic Brent Group in the North Sea. Morton analyzed garnet from the heavy mineral fractions of the Brent Group sandstones and compared the data to analyses of garnet from metamorphic terrains that previous studies indicated were suspected source areas. He identified garnet composition assemblages in the Brent Group

sandstones and found similar assemblages these source areas. Morton's conclusions are consistent with accepted models of Brent Group sedimentation.

I have compared my data to a collection of garnet compositional analyses compiled by Wright (1938) to determine, in a general sense, which types of terrains may have contributed sediment to the Munising Formation. Using Wright's data collection and ternary diagrams I distinguished compositional fields that correlate to different rock types. For each of the rock types, I drew boundaries base on Wright's data compilation that represents the composition of garnets derived from these rock types. I will use these boundaries to represent garnets from the corresponding rock type.

One of the ternary diagrams (Figure 35) is composed by representing common garnet end-members at three of the apexes. Figures 32, 33 ,34, 36, 37, have two garnet end-members at the bottom apexes and the top combines the other three garnet end-members. Wright originally composed ternary diagrams to graphically show the dominant end member composition of garnets from selected igneous and metamorphic rocks.

Interpretations

Garnets collected from the Munising Formation are dominantly almandine-pyrope type garnets (Table 5, Appendix 2). A comparison between the Munising garnet composition data and garnet composition data from pegmatites and granites (Figure 32) shows a fairly good correlation in almandine and pyrope content. Garnets collected from pegmatites and granites are dominantly almandine/spessartine. The pyrope/grossular/andradite (PGA) content is dominantly below 20%. However, the PGA content can be as high as 50% for low-spessartine garnets. The Munising garnets compositions are dominantly less than 10% spessartine and range from 10% to 77% almandine. Those garnets that contain greater than 70% almandine or contain some percentage of spessartine may have come from pegmatites or granitic source rocks.

Figures 33 and 34 show correlations between garnets from biotite and amphibole schists and the Munising garnets. The biotite garnets fall below 35% pyrope and not less than 60% almandine. Approximately one-third of the Munising garnets fall in the biotite schist field. The boundaries for garnets taken from amphibole schists are marked between 5% and 35% grossular and between 50% and 95% almandine. The Munising garnets

are distinctly low in grossular but many do fall within the approximated boundaries.

Garnet composition data from basic igneous rocks are plotted on a pyrope-almandine-grossular ternary (Figure 35) and form a field in the area of less than 35% grossular with a wide range in the composition of pyrope and almandine. Many of the Munising garnets fall within this field, suggesting a possible basic igneous source terrains for Munising garnets.

The Munising garnets are most likely not derived from contact metamorphic rocks. The Munising data do not fall in the field defined by the composition of garnets taken from contact metasiliceous rocks (Figure 36). Likewise the Munising garnets are not derived from eclogites, kimberlites, or peridotites (Figure 37). I did not plot the Munising garnet data on Wright's Figure 8 (a ternary with pyrope/spessartine/almandine, andradite, grossular apexes) because there is no correlation; this is obvious just by comparing the data Table 5 (or Appendix 2) with the figure. The highest percentage of andradite and grossular present in the Munising samples are 6.68 and 24.84 respectively. Garnets from calcareous rocks contain higher percentages of either andradite or grossular and less than 20% pyrope/spessartine/almandine.

Limitations

Morton (1985) presents an excellent review of the limitations in using heavy minerals to characterize the source rocks of a sandstone. The factors that can alter an initial garnet assemblage are, briefly:

- 1) multicycle sedimentation and hence multiple provenance; 2) heavy minerals are subject to dissolution in the weathering environment; and 3) intrastratal dissolution. Sandstones generally represent multiple cycles of sedimentation. Therefore, garnets present in sandstones can potentially represent any metamorphic source that served as a provenance for earlier sedimentation episodes. The Munising sandstones probably contain reworked sediments from the Jacobsville Sandstone which has abundant garnet (Hamblin, 1958). A provenance investigation of the Munising using garnet composition may actually give the provenance for the Jacobsville.

In preceding chapters I discussed intrastratal dissolution of garnet in the diagenetic environment. The tiny imbricate wedge marks on garnets in enlarged pore spaces are evidence that some garnet has been removed. There is no way to be certain that garnet dissolution was selective to a particular composition. Because of this uncertainty there is a possibility that

garnets of a specific composition were preferentially removed, in effect concentrating the more stable garnets compositions. Ternary diagrams composed using the resultant composition data could be biased to only the stable garnet compositions and may not represent the garnets derived from the source area.

In my interpretation of the Munising provenance garnet dissolution is apparent. However, it is of such small extent, and textural evidence gives no indication that entire grains have been removed. Therefore, I assume that garnet compositions in the Munising have not significantly altered since the garnets were removed from their initial source rocks.

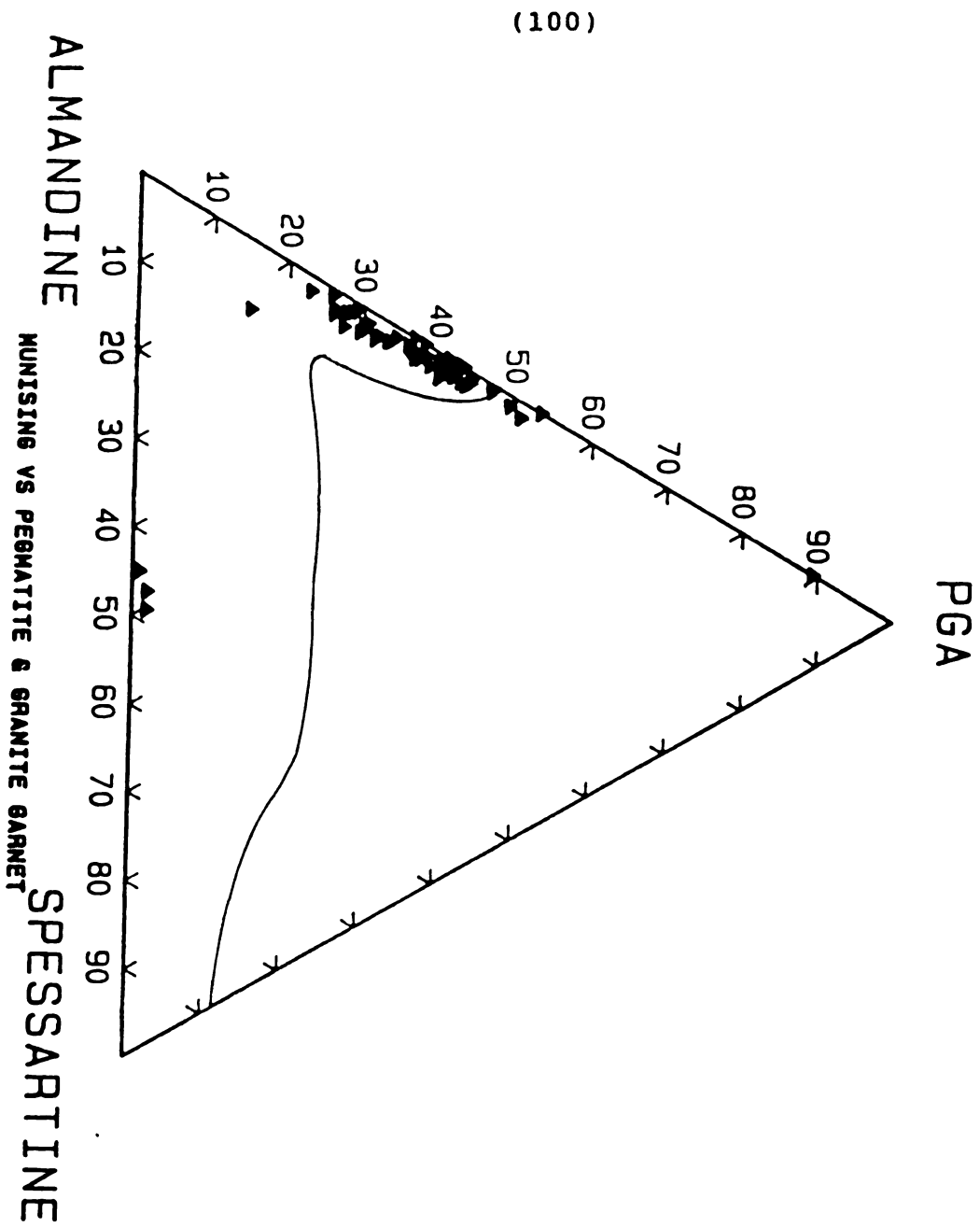


Figure 32. Munising vs. Pegmatite and Granite Garnet

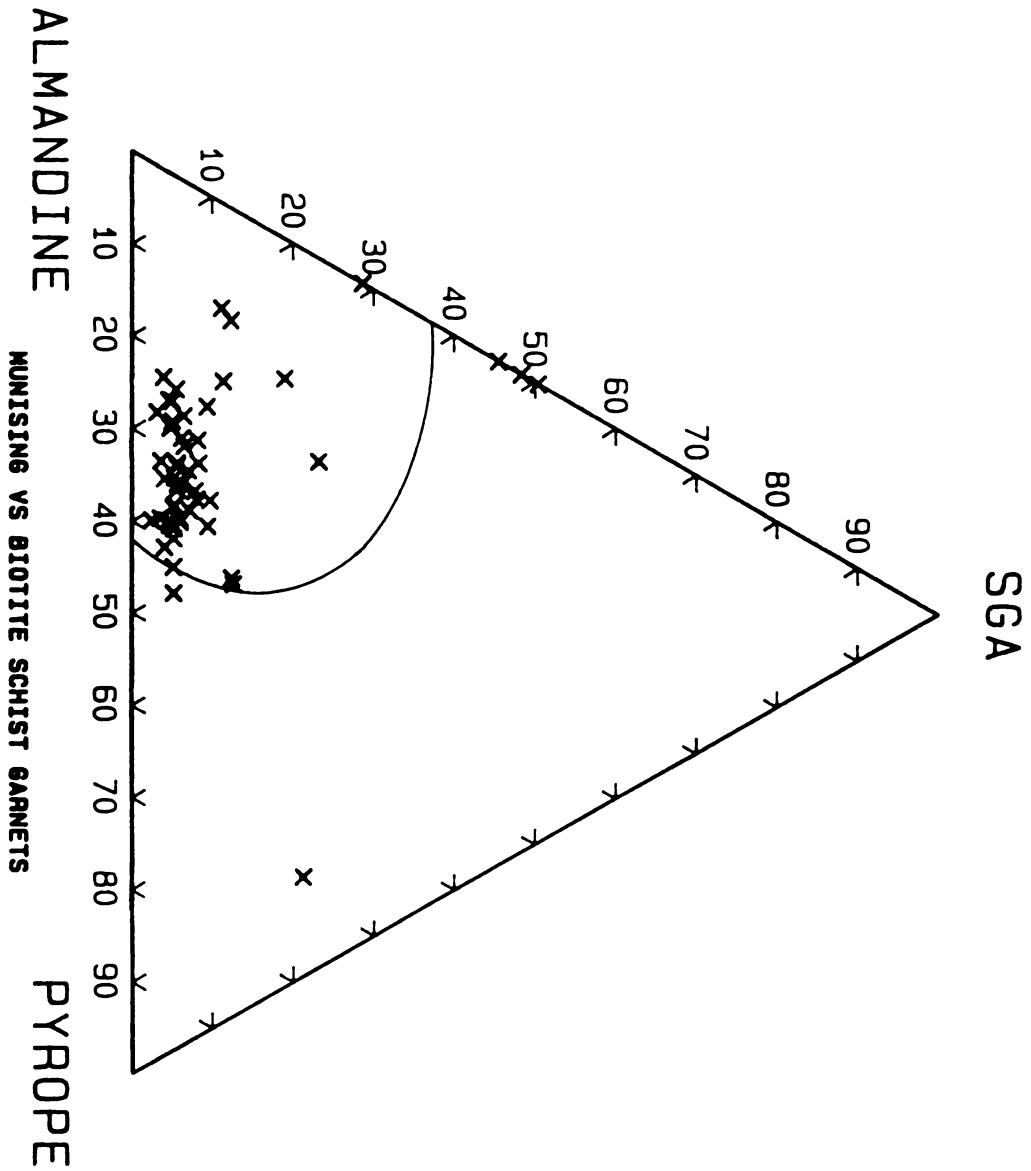


Figure 33. Munising vs. Biotite Schist Garnet

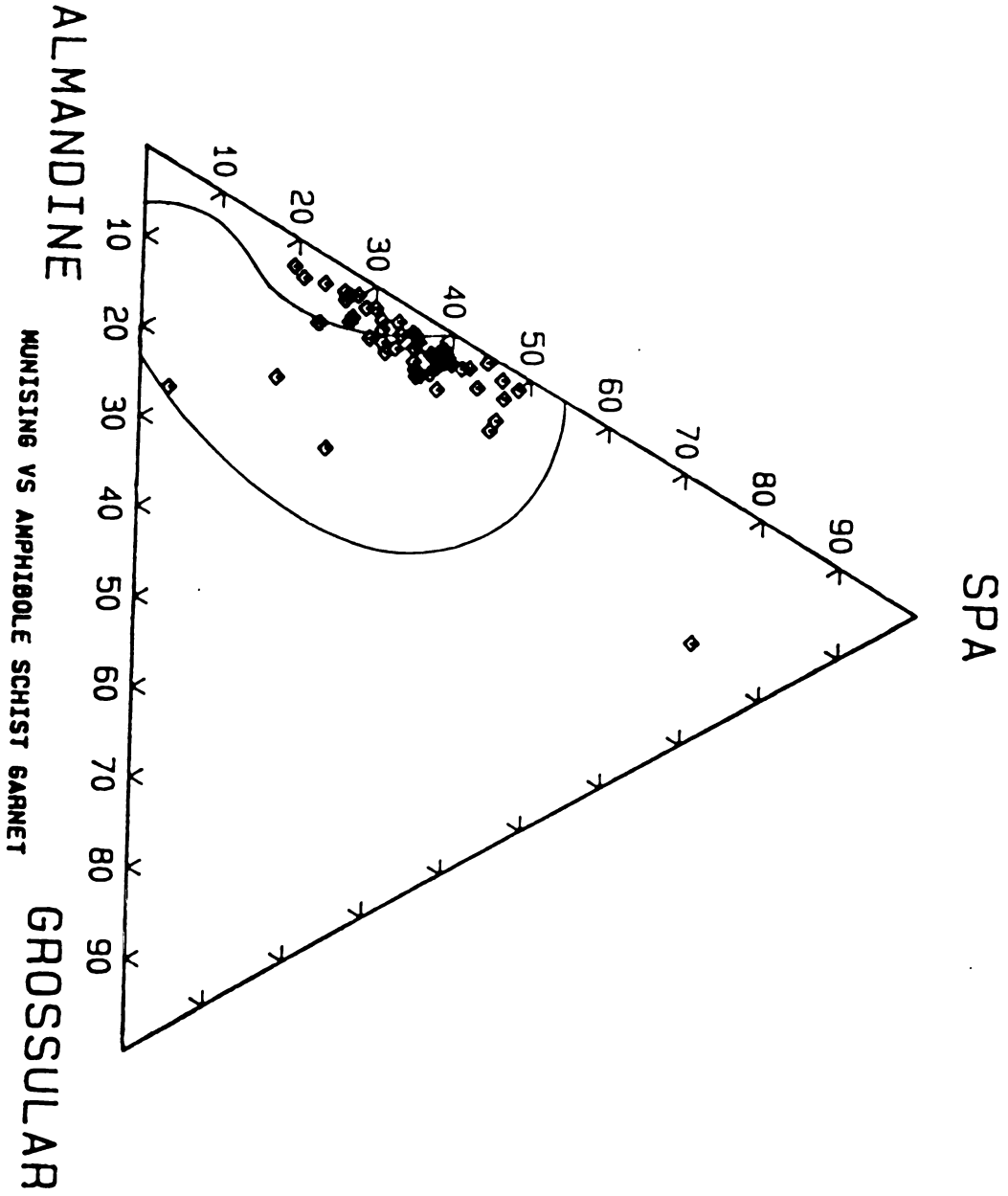


Figure 34. Munising vs. Amphibole Schist Garnet

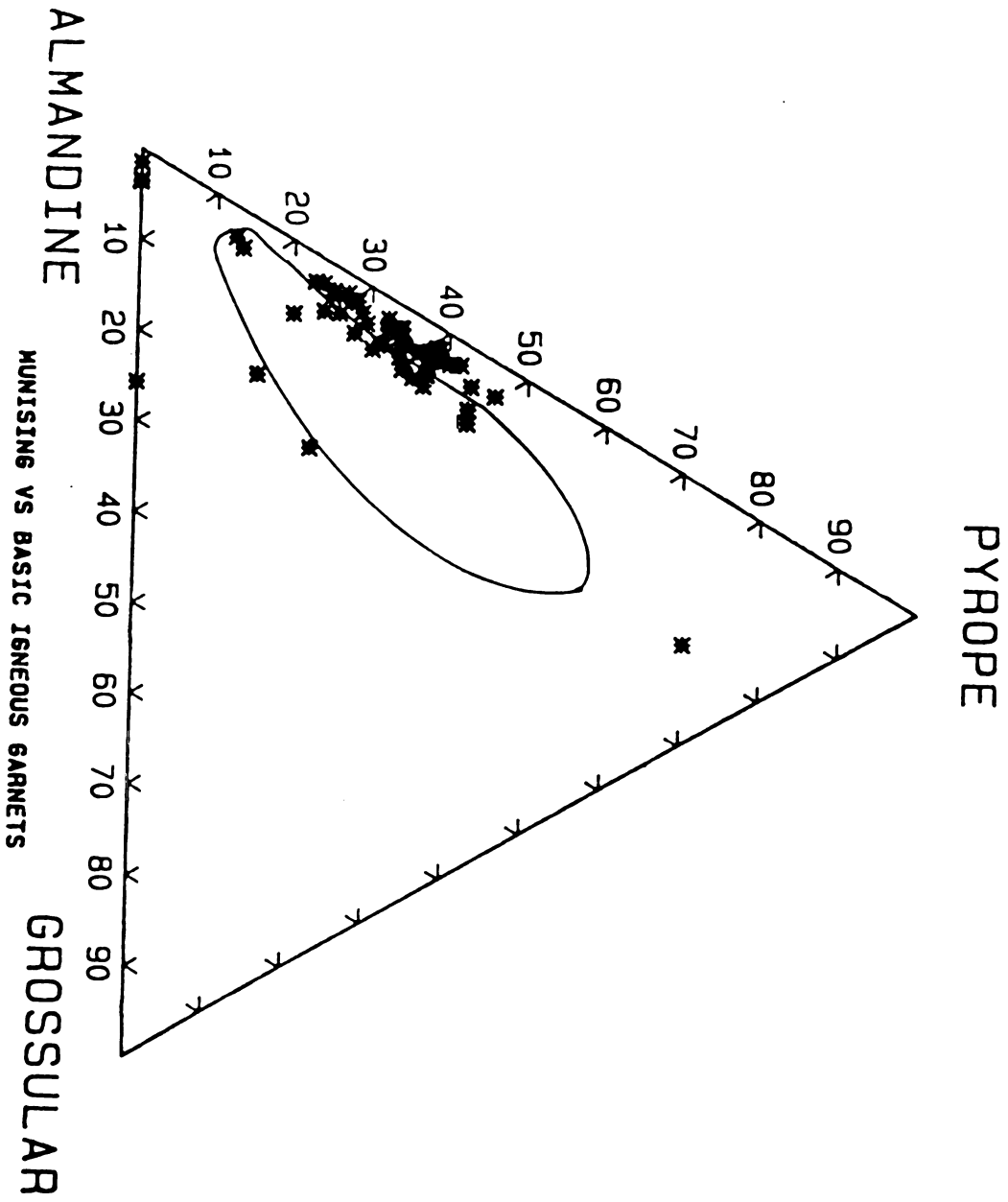


Figure 35. Munising vs. Basic Igneous Garnet

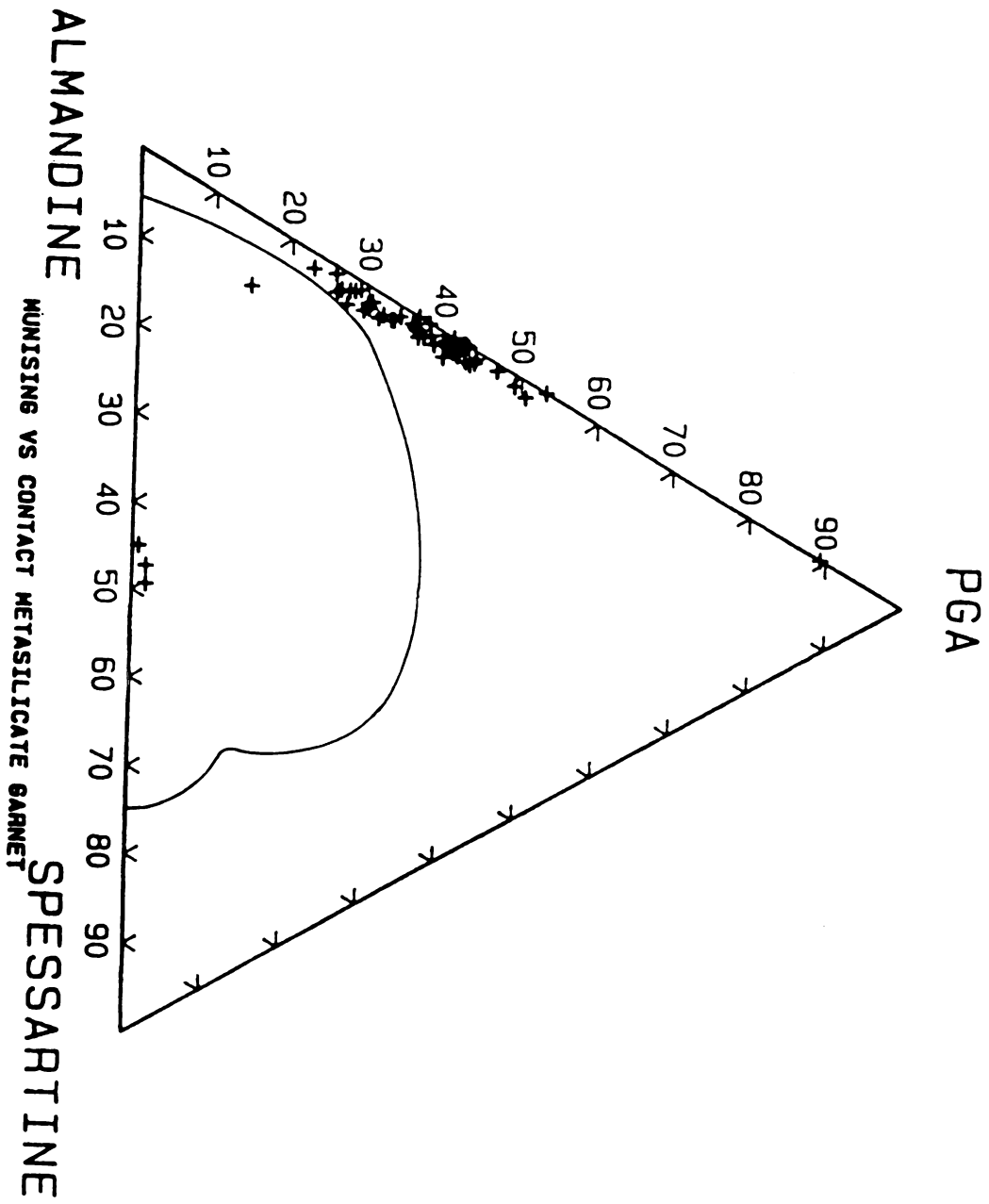


Figure 36. Munising vs. Contact Metasilicate Garnet

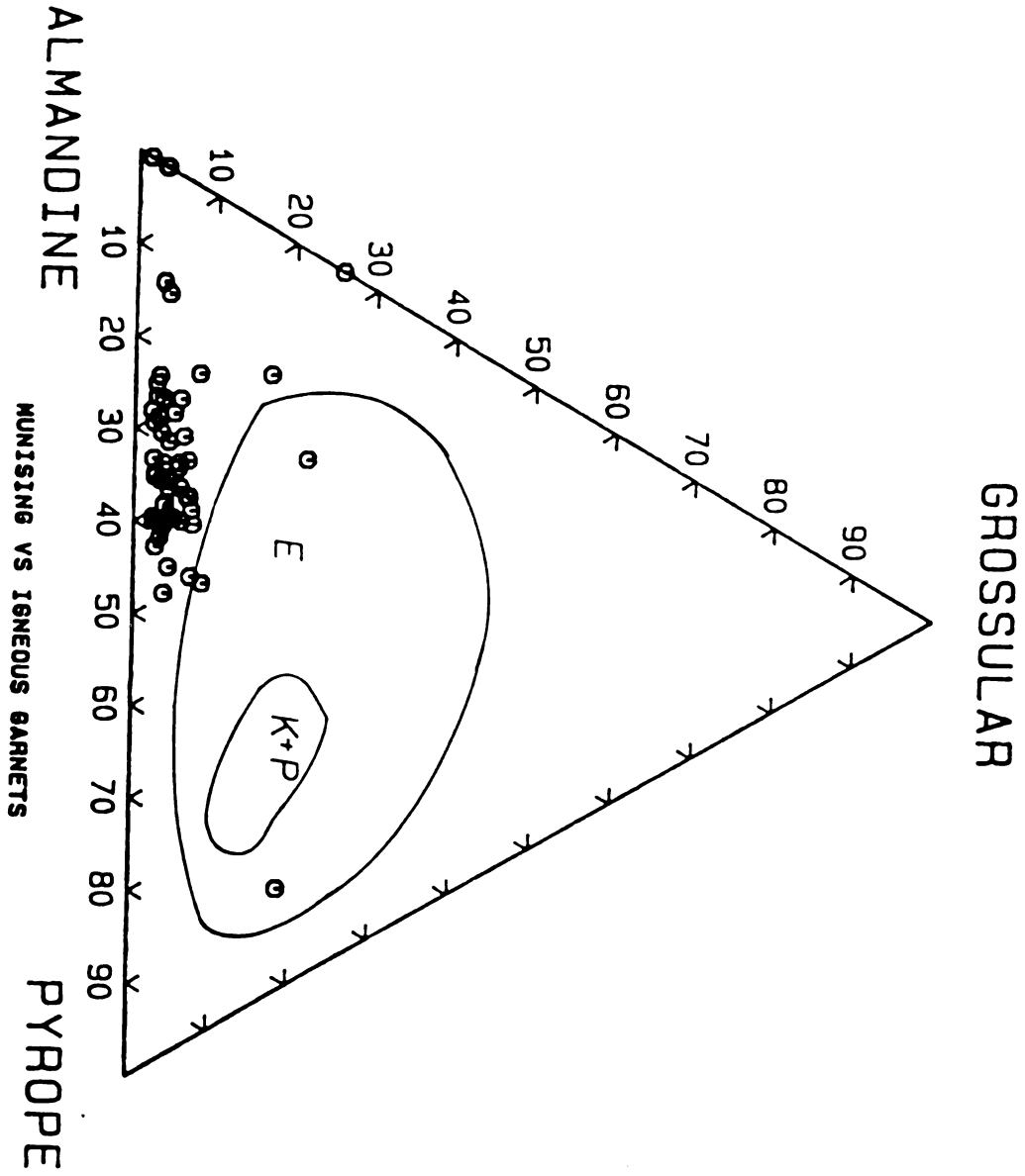


Figure 37. Muinsing vs. Igneous Garnet (Eclogites, Kimberlites and Peridotites)

THE PARAGENETIC SEQUENCE IN THE MUNISING FORMATION

The paragenetic sequence in the Munising Formation varies stratigraphically and, to a lesser degree, regionally. In general, the paragenetic sequence in the Munising Formation begins with mechanical compaction of the sediments. Formation of syntaxial authigenic potassium feldspar began contemporaneously with compaction. Depending on the sample, either calcium carbonate or quartz cement precipitated in the pore space. Quartz overgrowths developed after the potassium feldspar, and in the few examples containing both quartz and dolomite cemented sands, the quartz overgrowths formed prior to the dolomite.

Dolomite typically precipitated in the Munising sandstones as a pore lining and pore filling cement. When calcite is present, it occurs as a late stage pore filling cement. Crystallographically controlled garnet dissolution occurs after quartz and dolomite cementation and before calcite and mosaic silica cementation. Petrographic evidence does not clearly indicate when authigenic clay minerals formed in the sequence; however, it probably occurred after the feldspar overgrowths.

(107)

The last phase in the sequence is the precipitation of pore lining, mosaic silica, or, in dolomite samples, pore filling calcite cement. Figure 38 show the relative timing of the precipitation of authigenic material after deposition.

PARAGENESIS OF THE MUNISING FORMATION

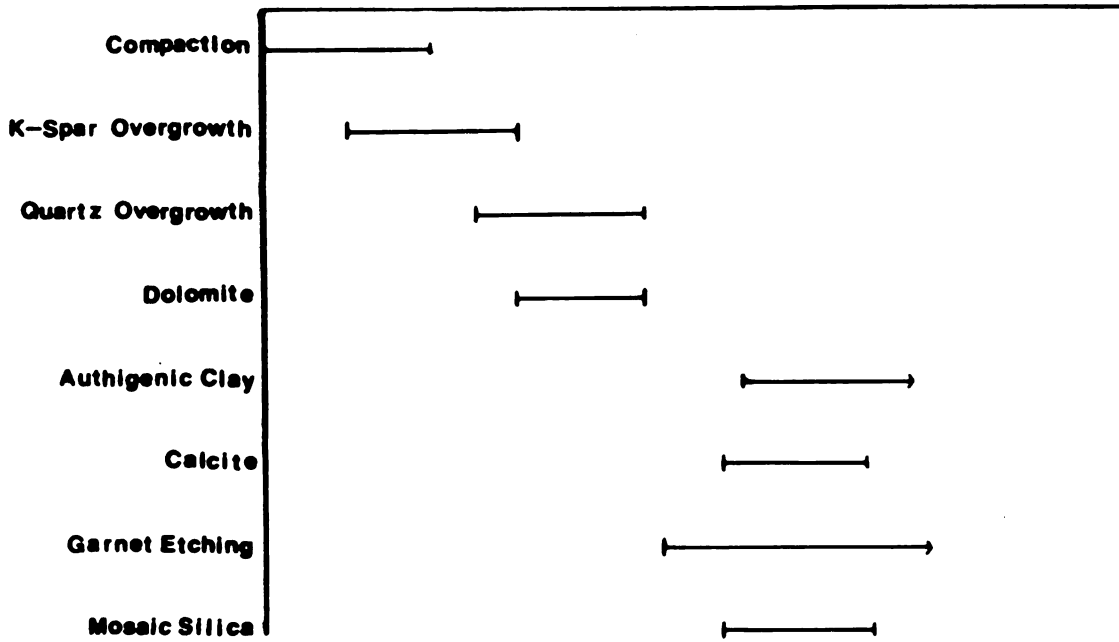


Figure 38. Summary of the paragenetic sequence in the Munising Formation

Discussion

Compaction in the Chapel Rock member was much more extensive than in the Miner's Castle member. The greater amount of compaction in the Chapel Rock may have been related to additional sediment deposition on this member. This sediment, if present, eroded away prior to the deposition of the Miner's Castle member, and may have induced the more extensive compaction found in these sandstones. The greater degree of compaction in the Chapel Rock member lends support to the postulated unconformity (Hamblin, 1958) between it and the Miner's Castle member. This can be added to the observations made by Hamblin (1958) and Driscoll (1959) that led them to conclude that there is an unconformity between the Miner's Castle member and the Chapel Rock member. Their evidence included mud cracks, differences in sedimentary structures, and heavy mineral assemblages. Whether the existence of the unconformity can be proven or not, the Chapel Rock has been subjected to more intense compaction and perhaps a more intensive diagenetic history than the sands of the Miner's Castle.

Authigenic syntaxial potassium feldspar formed contemporaneously with mechanical compaction. In every

case overgrowths are euhedral on detrital potassium feldspar. The ubiquitous presence of these overgrowths suggests that the pore fluids, shortly after deposition of the sand, had a high concentration of potassium and silica, and that dissolved aluminum was present.

Quartz overgrowths formed after the potassium feldspar which suggests that the pore fluids remained high in silica but became depleted in either aluminum or in potassium, or there was a change in the pH of the fluids.

Another possibility is that the quartz and potassium feldspar overgrowths formed at the same time. Thin section evidence and textural relationships clearly show that the quartz overgrowths continued to form after the feldspar overgrowths. However, textures cannot show whether or not the two were contemporary. Stability field diagrams show that contemporaneous, simultaneous quartz and feldspar overgrowth formation is possible over a wide range of silica and potassium concentrations. The two types of overgrowths could have easily formed simultaneously in the sandstone.

The mosaic silica precipitation event did not last long as indicated by textural evidence. Silica completely filled only the smallest pore spaces, such as those

formed by intrastratal dissolution of garnet and between quartz overgrowths, and formed only linings in the larger pores.

Carbonate cement is present in samples adjacent to the quartz cemented sandstones and as pods and lenticular bodies that crosscut primary sedimentary structures. This suggests that the dolomite formed independently of the quartz. The dolomite post dated the formation of the quartz overgrowths as indicated by the textures at quartz-carbonate contacts. The carbonate cement could have precipitated either long after or immediately after the quartz overgrowths as a pore lining and pore filling cement.

Secondary porosity is present in the Munising Formation in a minor, perhaps insignificant, amount. This diagenetic porosity is the result of dissolution of detrital feldspars and garnets. It is not apparent from textural evidence when the dissolution of feldspar took place. The delicate imbricate wedge marks found on garnets in every sample of the Munising Formation could not have formed prior to deposition because the marks are not rounded, fractured, or broken. Garnets are associated with enlarged pore spaces in both quartz-cemented sands and dolomite-cemented sands. Late diagenetic, pore lining, mosaic silica cement and

(112)

late calcite cement are found in the enlarged pore spaces adjacent to garnet in quartz cemented sandstones. The presence of these cements in the pore spaces around garnet suggests dissolution occurred after quartz and carbonate cementation, and prior to mosaic silica cementation.

**GARNET DIAGENESIS AND POSSIBLE IMPLICATIONS TO
PALEO-PORE FLUID CHEMISTRY**

The surface features discussed in the garnet diagenesis section may be useful in understanding the type of pore fluids that were present in the Munising Formation. However, before assumptions can be made about the paleo-pore fluids, laboratory experiments must identify what causes these surface textures. Once a fluid is identified as the cause in the laboratory it must be shown that the presence of this fluid in the Munising Formation is geologically reasonable. In the following paragraphs I review the laboratory experiments that attempted to reproduce garnet surface textures, field observations of the occurrence of garnet dissolution textures and a possible scenario to explain the presence of these features in the Munising.

Laboratory Attempts to Produce Wedge Mark Textures

Gravenor and Leavitt (1981) attempted to reproduce the etch features found on garnets in nature. This experiment was originally run by Bramlette (1929); however, there were no photographs or drawings to support his conclusion that the natural wedge marks features could be replicated. The purpose of Bramlette's (and later Gravenor's and Leavitt's)

experiments was to prove that the wedge marks on garnet were the result of etching. Crushed garnets of known composition were subjected to HF and NaOH solutions of varying concentration for varying lengths of time. Gravenor and Leavitt (1981) produced etch features on garnet similar to natural ones by dissolution in HF. Garnet etching took place within a short period of time (within 24 hours in 40% HF). The wedge marks are not exact replicas of natural wedge marks, but they are similar enough to prove that the wedge marks can be produced in the laboratory.

Because Rahmani (1973) deduced that basic solutions cause garnet wedge marks, Gravenor and Leavitt tried to replicate McMullen's (1959) experiment in which wedge marks were produced with NaOH. In the laboratory, NaOH solutions with varying concentrations etch grains; however, the surface textures formed were frosted garnets and not imbricate wedge marks. For whatever reason, Gravenor and Leavitt failed to reproduce the textures McMullen created using NaOH. Gravenor and Leavitt used garnets varying in composition, but they did not use the high spessartine as did McMullen. Their results were inconclusive as to whether basic solutions could cause wedge marks.

Hansley (in press) also tried to reproduce the natural wedge mark surface features on garnet. Instead of using strong acids, Hansley used organic acids of varying pH. Hansley, like Gravenor and Leavitt, placed crushed garnets of known composition into varying solutions. The solutions used were: one percent oxalic acid at pH 2, 6, and 8; one percent acetic acid at pH 3, 6, and 8; and humic and fulvic acids at pH values of 3, 5.5, and 8. Garnet etching only occurred in oxalic acid at the lowest pH. The surface textures on these garnets showed coalescing etch pits that formed features "identical" to natural facets (Hansley, in press).

Only in oxalic acid at pH 6 were any other surface features produced. These features were V-shaped pits which indicated dissolution was taking place. The acetic acid and the humic/fulvic acid solutions did not produce any features resembling wedge marks. These results led Hansley to conclude that garnet etching had a two fold dependency. 1) Dissolution is dependent on the anion in the organic acid, since the experiments use solutions of similiar pH. The fact that oxalate produced wedge marks suggests that dicarboxlytic organic acid anions rather than monofunctional organic acid anions cause garnet wedge marks (Hansley, in

press). 2) The pH variation in the oxalic acid solution led Hansley to conclude that garnet etching is also dependent on the hydrogen ion concentration in solution.

Related Surface Textures on Garnet

Another related occurrence of the surface textures is etch pits on garnets in the soil zone. As stated before, the dissolution features found on garnets in the soil zone (Velbel, 1984) are not morphologically similar to the wedge marks found on garnet in the Munising Formation. The presence/absence relationship between the garnet pitting and organic solutions in soils is similar to Hansley's suggestion that the formation of wedge marks on garnets in sandstones is dependent on organic acids. Also, Hansley showed that there is a relationship between the specific type of organic anion and the formation of the wedge marks.

Apatite and Garnet Assemblages

The presence of apatite in sandstones with wedge marked garnets features seems to be a recurring problem. Relative mineral stability tables such as Pettijohn (1941), Boswell (1942), Raeside (1959), and Morton (1984), show that apatite and garnet have

similar relative stabilities. The field evidence of Morton (1984), Borg (1986), Rahmani (1973), and Hansley (in press) also show that garnet and apatite are present together. However, Nickel (1973) shows that apatite at low pH (0.2 and 3.6) is highly soluble, even more so than almandine garnet. Sandstones that contain garnets with wedge marks are thought to have been exposed to solutions of low pH because low pH solutions are the only solutions thought to be capable of dissolving garnet.

If acidic solutions are invoked to explain the wedge mark formation, the presence of apatite needs to be explained. Because apatite and wedge marks on garnet were found in the heavy mineral assemblages of sandstones in Alberta, Rahmani (1973) suggests that the solutions were basic and not acidic. Thus, Rahmani's interpretation allows apatite and wedge marks to coexist. His interpretations seem flawed. The relative stabilities of these two minerals indicates that if dissolution occurs on garnet then it should also occur on apatite. If, as Nickel (1973) asserts, garnets are stable in basic solutions; what does Rahmani invoke as causing the etch features?

Hansley (in press) explains the coexistence of garnet wedge marks and apatite by considering the etching

solution acidic, and invoking high phosphorous content to explain the preservation of apatite. Hansley reports good evidence of high phosphorous activity in the Morrison Formation which is the result of organic material maturation and silicification of skeletal material. Other sandstones, however, in which apatite and wedge marked garnets occur (including the Munising Formation) do not show indications of high phosphorous content. Morton (1984) and Borg (1986) both recognized apatite along with etched garnets, but did not attempt to explain this coexistence by describing the solution pH or composition.

Morton (1986) addresses apatite dissolution as a function of depth in North Sea Jurassic sandstones. It was determined that apatite could exist in deep basin sandstones. Using core data, Morton determine that apatite etching occurred when the sandstone was exposed to meteoric water. Morton (1986) makes the implication that when garnets are etched apatite remains stable this is not consistent with Nickel (1973) conclusion.

In my work I am also faced with explaining the occurrence of apatite and wedge marks. There is evidence for apatite in the Munising sandstones. Hamblin (1958) includes it as a minor constituent of the heavy mineral fraction in the Chapel Rock member.

I have not identified apatite in petrographic or SEM grain mounts presumedly because of the much greater abundance of garnet in my heavy mineral samples. Even though I did not identify it, I consider it part of the Munising heavy mineral assemblage. The presence of apatite and wedge marks garnets appears to be due to selective preservation of the minerals.

Another observation that supports selective mineral preservation is the occurrence of carbonate with etched garnets. Even if apatite is not present in the sandstones I must account for the presence of dolomite cements. The garnet dissolution has occurred after quartz and, more significantly, dolomite cementation, as indicated by textural evidence. Also, Borg proposed a correlation between 1) apatite and wedge marks and 2) the presence of calcite cement. If acidic solutions were present in the sandstone after cementation, the carbonate minerals would be unstable and should show dissolution features. I have not observed the dissolution textures (Burley and Kantorowicz, 1986) on the carbonate cement.

A scenario can be developed that may explain occurrence of garnet wedge marks and apatite grains, and describe the type of solution that may have caused the garnet wedge mark formation in the Munising formation.

Solutions may have been only slightly acid and organic. In a slightly acidic solution, garnet would be less stable than in a neutral solution; the ability of the organic acids anions to chelate the iron and aluminum would provide a sink for the iron or aluminum released from the garnets. Apatite would be preserved because 1) it is more stable at the mildly acidic pH value, 2) does not contain iron or aluminum, and therefore would not dissolve.

A likely organic acid for this is oxalic acid, a weak acid and a chelator of iron and aluminum. Hansley (in press) shows that oxalic acid does produce wedge marks on garnet at pH 2 and V-shaped etch pits at pH 6. Also, Graustein (1977) states that the chelation of iron and aluminum by the organic acids allows phosphorous to remain available in solution. This is because the iron and aluminum oxides, which adsorb phosphorous, do not form. Oxalic acid may prevent undersaturation with respect to apatite cations and could allow the preservation of apatite.

CONCLUSIONS

The paragenetic sequence in the Munising Formation shows a series of porosity reducing events and minor porosity enhancing events. The porosity reducing events (compaction, feldspar and quartz overgrowth, carbonate and silica cementation) effectively reduced the porosity in these sandstones to zero to two percent when present. Porosity enhancing events, such as feldspar and garnet dissolution, increase the porosity less than one percent.

The SEM-EDS compositional data on the garnets in the Munising Formation can be used to imply a provenance containing granites, and biotite and amphibole schists as source rocks for sediments that yielded the Munising sandstones.

Garnet dissolution occurred after compaction, and quartz and dolomite cementation. In cemented samples, garnet dissolution is evident by enlarged pore spaces around garnet grains which have delicate, wedge shaped surface textures. The abundant, presently uncemented sandstones in the Munising Formation show no sign of cement dissolution, but do show evidence of the garnet dissolution event.

Garnet dissolution features in the Munising sandstones indicate that garnet was unstable during the post quartz/carbonate cementing period, and prior to the mosaic silica feldspar cementing period. Laboratory experiments show that garnet etching occurs only upon exposure to inorganic and/or organic acids. The inorganic acids which cause garnet etching in the laboratory are not likely to be significant constituents of natural basin fluids. There is no textural evidence of dissolution that indicates the presence of strong inorganic acids in the Munising sandstones and therefore inorganic acids are not likely the cause of garnet dissolution. Therefore, I believe the possible pore fluids that caused the garnet etching are acidic, more specifically weak organic acids.

Organic solutions are suspected for two reasons:

1) Organic acids are present in the the modern day soil zone where garnet etching occurs; 2) Organic anions show a selective nature to dissolution. In the cemented sandstone garnets are etched but the surrounding dolomite is not. The limited evidence of apatite in the Munising, and evidence of apatite in other sandstones with garnet etching, suggests that the solutions are selective to the chemistry of garnet.

I believe that oxalic acid is a likely component of the paleo-pore fluids in the Munising and may be the cause of garnet dissolution. Oxalic acid is a weak acid, it is selective to iron and aluminum chelation, and in laboratory experiments this acid produces etch features on almandine garnets.

Future Studies

This study has correlated a particular sandstone paragenetic sequence with textural dissolution evidence to deduce a component and a possible pH range of the paleo-pore fluids. At this point the number of laboratory correlations between a solution and the resulting surface texture on heavy minerals are few. However, garnet surface textures have been reasonably correlated with certain solutions. A petrographic examination should include detailed descriptions or photographs of the heavy minerals in the sandstone. In future petrographic investigations, garnet textures might be used to imply a type of paleo-pore fluid. With detailed stratigraphic sampling, surface textures on heavy minerals can be more than a presence-absence indicator of a fluid they can be used to trace the route the fluid has taken through the sandstone. If surface textures on the heavy minerals vary throughout

the sandstone, the presence of the textures can define the path of the paleo-fluids.

This study did not attempt to investigate the nature of heavy mineral dissolution; rather it applied laboratory results to field observations. During my work I found out that there is still a need to run experiments before direct correlations between field and laboratory evidence can be made. More experiments are needed on reproducing garnet surface textures. I believe the next set of experiments should address the relative stability of naturally occurring groups of minerals by exposure under laboratory conditions to a wide variety of solutions. Experiments could be run on:

- 1) Pairs of heavy minerals
- 2) Heavy minerals and different cement combinations
- 3) Whole sandstone samples, which would also show effect of grain packing on mineral dissolution.

These experiments are aimed at reproducing the textures on heavy minerals in sandstones so that a better correlation can be made between the observed surface textures and the paleo-pore solutions that cause the texture.

LIST OF REFERENCES

LIST OF REFERENCES

Adams, W.L. (1964) Diagenetic aspects of Lower Morrowan, Pennsylvania sandstones, Northwestern Oklahoma. *American Association of Petroleum Geologists Bulletin*, 48, 1568-1580.

Allen, J.R.L. (1962) Petrology, origin and deposition of the highest Lower Old Red Sandstone of Shropshire England. *J. sedim. Petrol.* 32, 657-697.

Bergquist, S.G. (1920) Stratigraphy of Alger County. Michigan Geological Survey Division Cambrian Data Collection.

Borg, G., (1986) Faceted garnets formed by etching. Example sandstones of Late Triassic, South Germany. *Sedimentology*, 33, 141-146.

Boswell, P.H.G. (1942) The stability of minerals in sedimentary rocks. *Quart. J. geol. Soc. London*, 97, 56-75.

Bramlette, M.N. (1929), Natural etching of detrital garnet. *Am. Mineralogist*, 14, 336-337.

Burley, S.D. & Kantorowicz, J. D. (1986) Thin section and S.E.M. textural criteria for the recognition of cement-dissolution porosity in sandstones. *Sedimentology*, 33, 587-604.

Cohee, G.V. (1945) Stratigraphy of Lower Ordovician and Cambrian rocks in the Michigan Basin. U.S.G.S. Oil and Gas Investigation. Preliminary Chart no. 9.

Driscoll, E.G. (1959) Evidence of transgressive-regressive Cambrian sandstones bordering Lake Superior. *J. sedim. Petrol.* 29, 5-15.

Folk, R.L. (1975) Glacial deposits identified by chattermark trails in detrital garnets *Geology*, 3, 473-476.

Graustein, W.C. (1977) Calcium oxalate: Occurrence in soils and effect on nutrient and geochemical cycles. *Science*, 1252-1254.

Gravenor, C.P. & McIelwain T.A. & Stubausky, M. (1978) Chattermark trails and heavy minerals in glacial sediments. *Geology*. 25, 159-171.

Gravenor, C.P. & Leavitt, R.K. (1981) Experimental formation and significance of etch patterns on detrital garnets. *Can. J. Earth Sci.* 18, 765-775.

Gregg, J.M. & Sibley, D.F. (1984) Epigenetic dolomitization and the origin of xenotopic dolomite texture. *J. sedim. Petrol.* 54, 908-931.

Griffiths, J.M. (1967) *Scientific method analysis of sediments*. McGraw-Hill Book Co.; New York. 507pp.

Haddox, C.A. (1982) *Sedimentology of the Munising Formation*. M.S. Thesis, 194 pp.

Hamblin, W.K. (1958) *Cambrian Sandstones of Michigan*. Michigan Department of Conservation, Geological Survey Division, Publication 51, 146.

Hansley, P.L. (in press) Natural and experimental etching of garnets by organic acids; Etched garnets in the Upper Jurassic Morrison Formation, Northwestern New Mexico Evidence for organic-acid bearing solutions. *J. sedim. Petrol.*

Hemingway, J.E. & Tamar-Agha, M.Y. (1975) The effects of diagenesis on some heavy minerals from the sandstones of the Middle Limestone Group in Northumberland. *Yorkshire geol. Soc. Proc.* 40, part 4, no. 31, 537-546.

Kalliokoski, J.O. (1982) *Jacobsville Sandstone in Geology and Tectonics of the Lake Superior Basin.* Memoir of the Geological Society of America. 147-155.

Martin, H. (1957) *Geological Map of Michigan,* Michigan Department of Conservation.

McMullen, R.M. (1959) Etched detrital garnet from the Cardium Formation, Pembina area, Central Alberta *Alberta Soc. Petroleum Geologists, J.,* 7, 272-274.

Morton, A.C. (1979 a) Depth control of intrastratal solution of heavy minerals from the Paleocene of the North Sea. *J. sedim. Petrol.* 49, 281-286.

Morton, A.C. (1979 b) Surface features of heavy mineral grains from Paleocene sands of the Central North Sea. *Scottish J. geol.* 15, 293-300.

Morton, A.C. (1984) Stability of detrital heavy minerals in Tertiary sandstones from the North Sea. *Clay Miner.* 19, 287-308.

Morton, A.C. (1985) A new approach to provenance studies: electron microprobe analysis of detrital garnets from Middle Jurassic sandstones of the northern North Sea. *Sedimentology,* 32, 553-566.

Morton, A.C. (1986) Dissolution of apatite in North Sea Jurassic sandstones: Implications for the generation of secondary porosity. *Clay Miner.* 21, 711-733.

Nickel, E. (1973) Experimental dissolution of light and heavy minerals in comparison with weathering and intrastratal solution. *Contr. to Sedimentology,* 1, 1-68.

Odom, I.E. (1975) Feldspar-grain size relations in Cambrian arenites, Upper Mississippi Valley. *J. sedim. Petrol.* 45, 636-650.

Odom, I.E., Doe, T.W. & Dott, R.H. Jr. (1976) Nature of feldspar-grainsize relations in some quartz-rich sandstones. *J. sedim. Petrol.* 46, 862-870.

Odom, I.E (1978) Mineralogy of late Cambrian and early Ordovician sandstones Upper Mississippi Valley lithostratigraphy, petrology, and sedimentation of Late Cambrian and Early Ordovician rocks near Madsion, Wisconsin: Field Trip Guide Book, no. 3 Great Lakes SEPM 46-51.

Oetking, P.E. (1951) The relation of the Lower Paleozoic to the older rocks in the Northern Peninsula of Michigan Unpublished Ph.D. thesis, University of Wisconsin, Madison, Wisconsin.

Orr, E.D. & R.L. Folk (1983) New Scents on the Chattermark Trail: Weathering enhances obscure microfractures. *J. sedim. Petrol.* 53, 121-129.

Ostrom, M.E. (1967), Geologic cross section, Alger County, Michigan -- Walworth County, Wisconsin; Correlation problems of Cambrian and Ordovician outcrop areas, Upper Peninsula, Michigan: Michigan Basin Society, 36-41.

Pettijohn, F.J. (1941) Persistence of heavy minerals and geologic age. *J. Geology* 49, 610-625.

Pettijohn, F.J., Potter, P.E. & Siever, R. (1973) Sand and sandstones Springer-Verlag, New York, 618 pp.

Raeseide, J.D. (1959) Stability of index minerals in soils with particular reference to quartz, zircon and garnet. *J. sedim. Petrol.* 29, 493-502.

Rahmani, R.A. (1973) Grain surface etching features of some heavy mineral. *J. sedim. Petrol.* 43, 882-888.

- Schmidt, V. & McDonald, D.A. (1979 a) The role of secondary porosity in the course of sandstone diagenesis. In **Aspects of Diagenesis** (Ed. by P. A. Scholle and P. R. Schulger). Spec. Publ. Soc. econ. Paleont. Miner., No. 26, 175-207.
- Schmidt, V. & McDonald, D.A. (1979 b) Texture and recognition of secondary porosity in sandstones. In **Aspects of Diagenesis** (Ed. by P. A. Scholle and P. R. Schulger). Spec. Publ. Soc. econ. Paleont. Miner., No. 26, 209-225.
- Setlow, L.W. and Karpovich, R.P. (1972) "Glacial" microtextures on quartz and heavy mineral sand grains from the littoral environment. **J. sedim. Petrol.** 42, 864-875.
- Shaver, R.H. (1980) AAPG chart publication; Correlation of stratigraphic units of North America; Midwestern Basin and Arches region
- Sibley, D.F. (1978) Feldspar cement in the Jacobsville Sandstone **J. sedim. Petrol.** 48, 983-986.
- Simpson, G.S. (1976) Evidence of overgrowths on, and solution of detrital garnet. **J. sedim. Petrol.** 46, 689-693.
- Stablein, K.K. & E.C. Dapples (1977) Feldspars from the Tunnel City Group (Cambrian) Western Wisconsin. **J. sedim. Petrol.** 47, 1523-1538.
- Stieglitz, R.D. & Rothwell, B. (1978) Surface microtextures of freshwater heavy mineral grains. **Geoscience Wisconsin, Geological and Natural History Survey** 3. 21-34.
- Velbel, M.A., (1984) Natural weathering mechanisms of almandine garnet. **Geology**, 12, 631-634.

Wilson, M.D. & Pittman, E.D. (1977) Authigenic clays in sandstones: Recognition and influence on reservoir properties and paleoenvironmental analysis. *J. sedim. Petrol.* 47, 3-31.

Wright, W.I. The composition and Occurrence of garnet. *Am. Mineralogist*, 23, 436-439.

APPENDIX ONE
PETROGRAPHIC PRESENCE/ABSENCE CHART

PRESENCE/ABSENCE TABLE

SAMPLE	LOCATION	FORMATION	SORTING	GRAIN SIZE
10-25-S	1 LFW	MC	POOR	0.33
10-25-N	1 LFW	MC	POOR	0.35
10-25-O	1 LFW	MC	POOR	0.25
10-25-P	1 LFW	MC	POOR	0.26
10-25-C	1 LFW	MC	POOR	0.42
10-25-J	1 LFW	MC	POOR	0.3
10-25-Q	1 LFW	MC	POOR	0.32
10-25-D	1 LFW	MC	POOR	0.39
10-25-R	1 LFW	MC	POOR	0.34
09-21-B	2 MUN WEST	CH	POOR	0.34
09-21-A	2 MUN WEST	CH	POOR	0.28
10-26-A	2 MUN WEST	CH	MOD	0.34
10-25-A	3 WAG FALL	MC	POOR	0.41
10-26-H	4 TAN FALL	MC	MOD	0.5
09-21-I	7 MINER FALL	MC	POOR	0.36
09-21-E	7 MINER FALL	MC	WELL	0.36
09-21-F	7 MINER RIV	MC	POOR	0.37
09-21-H	7 MINER FALL	MC	MOD	0.53
09-21-G	7 MINER FALL	MC	POOR	0.47
10-26-M	9 MOS FALL	MC	POOR	0.33
10-26-L	9 MOS FALL	MC	POOR	0.34
10-26-I	10 CHAP ROCK	CH	MOD	0.18
10-27-A	11 LBL	CH	POOR	0.34
10-27-D	11 LAKE SUP	CH	POOR	0.1
10-27-E	11 LBL	CH	POOR	0.41
10-27-C	11 LBL	CH	POOR	0.18
10-27-H	11 LAKE SUP	CH	POOR	0.29
09-22-E	12 HURR RIV	MC	GOOD	0.39
09-22-F	12 HURR RIV	MC	MOD	0.39
09-23-D	13 TAQ FALL	CH	MOD	0.21

PRESENCE/ABSENCE TABLE

SAMPLE	DETRITAL	QUARTZ	CLAY	GARNET	ZIRCON
	KSP				
10-25-S	YES	YES	YES	YES	YES
10-25-N	YES	YES	NO	YES	NO
10-25-O	YES	YES	YES	YES	YES
10-25-P	YES	YES	NO	YES	YES
10-25-C	YES	YES	YES	YES	NO
10-25-J	YES	YES	YES	YES	NO
10-25-Q	YES	YES	NO	YES	NO
10-25-D	YES	YES	NO	YES	YES
10-25-R	YES	YES	NO	YES	NO
09-21-B	YES	YES	YES	NO	NO
09-21-A	YES	YES	YES	YES	NO
10-26-A	YES	YES	YES	NO	NO
10-25-A	NO	YES	YES	NO	NO
10-26-H	YES	YES	NO	YES	YES
09-21-I	YES	YES	NO	YES	NO
09-21-E	YES	YES	YES	YES	NO
09-21-F	YES	YES	NO	YES	NO
09-21-H	YES	YES	NO	YES	NO
09-21-G	YES	YES	NO	YES	NO
10-26-M	YES	YES	NO	YES	YES
10-26-L	YES	YES	NO	YES	NO
10-26-I	YES	YES	YES	NO	YES
10-27-A	NO	YES	YES	NO	YES
10-27-D	YES	YES	YES	NO	NO
10-27-E	YES	YES	YES	NO	NO
10-27-C	YES	YES	YES	NO	NO
10-27-H	YES	YES	NO	NO	NO
09-22-E	YES	YES	YES	YES	NO
09-22-F	YES	YES	YES	NO	NO
09-23-D	NO	YES	YES	NO	NO

PRESENCE/ABSENCE TABLE

SAMPLE	TOURMAL	DETRITAL CARB	ROCK FRAG	CEMENT	DOLOMITE
10-25-S	NO	NO	YES	CLAY	NO
10-25-N	NO	FOSSILS	YES	DOLO	YES
10-25-O	YES	NO	YES	NO	NO
10-25-P	NO	NO	YES	NO	NO
10-25-C	NO	NO	YES	NO	NO
10-25-J	NO	NO	NO	CLAY/IRON	YES
10-25-Q	NO	NO	YES	NO	NO
10-25-D	NO	NO	YES	DOLO	YES
10-25-R	NO	PELLETS	NO	QTZ DOL	NO
09-21-B	NO	NO	YES	MATRIX	NO
09-21-A	NO	NO	YES	MATRIX	NO
10-26-A	YES	NO	YES	MATRIX	NO
10-25-A	NO	NO	NO	QTZ	NO
10-26-H	NO	NO	YES	DOLO	YES
09-21-I	NO	NO	NO	DOLO	YES
09-21-E	NO	PELLETS	NO	QTZ	NO
09-21-F	NO	PELLETS	YES	DOLO	YES
09-21-H	NO	PELLETS	YES	CAR MTRX	NO
09-21-G	NO	NO	NO	DOLO	YES
10-26-M	NO	NO	YES	NO	NO
10-26-L	NO	NO	NO	QTZ	NO
10-26-I	YES	NO	YES	FRMWORK	NO
10-27-A	NO	NO	NO	FRMWORK	NO
10-27-D	NO	NO	YES	FRMWORK	NO
10-27-E	NO	NO	YES	CLAY	NO
10-27-C	NO	NO	YES	CLAY/FRMWORK	NO
10-27-H	NO	NO	YES	SIDERITE	NO
09-22-E	NO	NO	YES	IRON/CLAY	NO
09-22-F	NO	NO	YES	NO	NO
09-23-D	NO	NO	YES	MATRIX	NO

PRESENCE/ABSENCE TABLE

SAMPLE	POIKILOTOPIC DOLOMITE	PORE LINING DOLOMITE	PORE FILLING DOLOMITE	ANHEDRAL DOLOMITE
10-25-S	NO	NO	NO	NO
10-25-N	NO	NO	YES	YES
10-25-O	NO	NO	NO	NO
10-25-P	NO	NO	NO	NO
10-25-C	NO	NO	NO	NO
10-25-J	NO	NO	NO	NO
10-25-Q	NO	NO	NO	NO
10-25-D	YES	NO	NO	YES
10-25-R	NO	YES	YES	NO
09-21-B	NO	NO	NO	NO
09-21-A	NO	NO	NO	NO
10-26-A	NO	NO	NO	NO
10-25-A	NO	NO	NO	NO
10-26-H	NO	YES	NO	NO
09-21-I	NO	NO	YES	NO
09-21-E	NO	NO	NO	NO
09-21-F	NO	NO	YES	NO
09-21-H	NO	NO	NO	YES
09-21-G	NO	YES	YES	YES
10-26-M	NO	NO	NO	NO
10-26-L	NO	NO	NO	NO
10-26-I	NO	NO	NO	NO
10-27-A	NO	NO	NO	NO
10-27-D	NO	NO	NO	NO
10-27-E	NO	NO	NO	NO
10-27-C	NO	NO	NO	NO
10-27-H	NO	NO	NO	NO
09-22-E	NO	NO	NO	NO
09-22-F	NO	NO	NO	NO
09-23-D	NO	NO	NO	NO

PRESENCE/ABSENCE TABLE

SAMPLE	EUHEDRAL DOLOMITE	CALCITE	PORE FILLING CALCITE	QUARTZ OVERGROWTH
10-25-S	NO	NO	NO	NO
10-25-N	YES	YES	YES	NO
10-25-O	NO	NO	NO	NO
10-25-P	NO	NO	NO	NO
10-25-C	NO	NO	NO	NO
10-25-J	NO	NO	NO	NO
10-25-Q	NO	NO	NO	NO
10-25-D	NO	NO	NO	NO
10-25-R	YES	YES	YES	YES
09-21-B	NO	NO	NO	NO
09-21-A	NO	NO	NO	NO
10-26-A	NO	NO	NO	NO
10-25-A	NO	NO	NO	YES
10-26-H	YES	NO	NO	NO
09-21-I	YES	YES	NO	NO
09-21-E	NO	NO	NO	NO
09-21-F	YES	YES	NO	NO
09-21-H	NO	NO	NO	NO
09-21-G	YES	NO	NO	NO
10-26-M	NO	NO	NO	NO
10-26-L	NO	NO	NO	YES
10-26-I	NO	NO	NO	NO
10-27-A	NO	NO	NO	NO
10-27-D	NO	NO	NO	NO
10-27-E	NO	NO	NO	NO
10-27-C	NO	NO	NO	NO
10-27-H	NO	NO	NO	NO
09-22-E	NO	NO	NO	NO
09-22-F	NO	NO	NO	NO
09-23-D	NO	NO	NO	YES

PRESENCE/ABSENCE TABLE

SAMPLE	KSPAR OVERGROWTH	MOSAIC SILICA	AUTHIGENIC CLAY	HEMATITE STAIN	POROSITY
10-25-S	YES	NO	NO	YES	YES
10-25-N	YES	NO	NO	YES	NO
10-25-O	YES	NO	POSS	YES	YES
10-25-P	YES	NO	NO	YES	YES
10-25-C	YES	NO	POSS	NO	YES
10-25-J	YES	NO	POSS	YES	YES
10-25-Q	YES	NO	NO	NO	YES
10-25-D	YES	NO	NO	NO	NO
10-25-R	YES	YES	NO	NO	YES
09-21-B	YES	NO	POSS	YES	NO
09-21-A	YES	NO	POSS	YES	NO
10-26-A	YES	NO	POSS	YES	YES
10-25-A	NO	NO	POSS	YES	YES
10-26-H	YES	NO	NO	NO	YES
09-21-I	YES	NO	NO	NO	NO
09-21-E	YES	YES	POSS	NO	YES
09-21-F	YES	NO	NO	YES	NO
09-21-H	YES	NO	NO	YES	NO
09-21-G	YES	NO	NO	NO	NO
10-26-M	YES	NO	NO	YES	YES
10-26-L	YES	YES	NO	NO	NO
10-26-I	YES	NO	POSS	NO	YES
10-27-A	NO	NO	POSS	NO	YES
10-27-D	YES	NO	POSS	NO	YES
10-27-E	YES	NO	POSS	YES	YES
10-27-C	YES	NO	POSS	YES	YES
10-27-H	YES	NO	NO	YES	NO
09-22-E	YES	NO	POSS	YES	YES
09-22-F	YES	NO	POSS	YES	YES
09-23-D	NO	NO	POSS	YES	YES

PRESENCE/ABSENCE TABLE

SAMPLE	BROKEN KSPAR	STYOLITES	PRESSURE SOLUTION	DEFORMED PHYLLOSILCATES	ALTERED KSP CORES
10-25-S	NO	NO	NO	NO	YES
10-25-N	NO	NO	NO	NO	NO
10-25-O	NO	NO	NO	NO	YES
10-25-P	NO	NO	NO	NO	YES
10-25-C	NO	NO	NO	NO	NO
10-25-J	NO	NO	NO	NO	NO
10-25-Q	NO	NO	NO	NO	YES
10-25-D	NO	NO	NO	NO	NO
10-25-R	NO	NO	NO	NO	NO
09-21-B	YES	NO	YES	YES	YES
09-21-A	NO	NO	YES	YES	YES
10-26-A	YES	NO	NO	YES	YES
10-25-A	NO	NO	NO	NO	NO
10-26-H	NO	NO	NO	NO	NO
09-21-I	NO	NO	NO	NO	NO
09-21-E	NO	NO	NO	NO	YES
09-21-F	NO	NO	NO	NO	YES
09-21-H	NO	NO	NO	NO	NO
09-21-G	NO	NO	NO	NO	NO
10-26-M	YES	NO	NO	NO	NO
10-26-L	NO	NO	NO	NO	YES
10-26-I	NO	NO	YES	YES	NO
10-27-A	YES	YES	YES	NO	NO
10-27-D	NO	YES	YES	NO	NO
10-27-E	NO	NO	YES	NO	NO
10-27-C	NO	YES	YES	NO	NO
10-27-H	NO	NO	NO	NO	YES
09-22-E	NO	NO	NO	NO	NO
09-22-F	NO	NO	YES	NO	NO
09-23-D	NO	YES	YES	YES	NO

PRESENCE/ABSENCE TABLE

SAMPLE	ALTERED KSP CORES+OVG	ENLARGED PORE SPACE	GARNET WEDGE MARKS
10-25-S	NO	NO	NO
10-25-N	NO	YES	YES
10-25-O	YES	NO	YES
10-25-P	YES	NO	YES
10-25-C	NO	NO	NO
10-25-J	NO	NO	YES
10-25-Q	NO	NO	YES
10-25-D	NO	YES	YES
10-25-R	NO	YES	YES
09-21-B	NO	NO	NO
09-21-A	YES	NO	NO
10-26-A	NO	YES	NO
10-25-A	NO	NO	NO
10-26-H	NO	NO	NO
09-21-I	NO	NO	NO
09-21-E	NO	YES	YES
09-21-F	NO	NO	NO
09-21-H	NO	NO	NO
09-21-G	NO	NO	YES
10-26-M	NO	NO	NO
10-26-L	NO	YES	YES
10-26-I	NO	NO	NO
10-27-A	NO	NO	NO
10-27-D	NO	NO	NO
10-27-E	NO	YES	NO
10-27-C	NO	NO	NO
10-27-H	NO	NO	NO
09-22-E	NO	NO	NO
09-22-F	NO	NO	NO
09-23-D	NO	NO	NO

APPENDIX TWO

**MOLE PERCENT OF GARNET END-MEMBERS
FOR MUNISING GARNET GRAINS**

APPENDIX 2
TABLE 1
MOLE PERCENT END-MEMBERS

SAMPLE	RUN	SPSS- ARTINE	ALMA- DINE	PYROPE	GROSS- ULAR	ANDRA- DITE
10-25-N	1	1.25	64.62	31.73	2.40	0
10-25-N	2	2.90	65.82	27.96	3.33	0
10-25-N	3	3.53	69.38	19.29	7.81	0
10-25-N	4	2.91	57.34	32.96	6.79	0
10-25-N	5	2.10	64.60	27.22	6.08	0
10-25-N	6	2.36	61.16	33.20	3.28	0
10-25-C	1	1.82	70.71	24.70	2.76	0
10-25-C	2	44.97	55.03	0	0.85	0
10-25-C	3	0.90	59.05	35.68	3.85	0.51
10-25-C	4	46.40	51.74	0	1.86	0
9-21-C	1	1.45	62.52	33.43	2.60	0
9-21-C	2	1.51	68.07	25.49	4.93	0
9-21-C	3	1.26	60.55	33.87	4.32	0
9-21-C	4	2.13	59.31	32.85	5.71	0
9-21-C	5	2.24	65.76	15.15	16.64	0
10-25-Q	1	1.50	58.86	34.02	5.62	0
10-25-Q	2	1.10	58.55	37.95	2.41	0
10-25-Q	3	1.40	58.86	36.03	3.71	0
10-25-Q	4	0.83	57.25	36.90	5.03	0
10-25-Q	5	0	58.83	38.73	2.44	0
10-25-S	1	48.46	49.66	0	1.88	0
10-25-S	2	0	62.04	32.67	2.63	2.66
10-26-E	1	2.27	64.80	28.67	4.26	0
10-26-E	2	0.81	52.39	42.44	4.36	0
10-26-E	3	7.91	77.37	11.49	3.22	0
9-21-H	1	1.28	63.04	31.34	3.63	0.71
9-21-H	2	1.18	57.17	36.83	4.81	0
9-21-H	3	2.49	67.63	27.45	2.43	0
9-21-H	4	2.21	71.43	0	24.84	1.52
10-26-L	1	2.36	67.69	27.52	2.43	0
10-26-L	2	0	57.20	38.13	3.79	0.88
10-26-L	3	1.56	61.87	31.06	5.51	0
10-26-L	4	0	63.41	30.94	5.65	0
10-25-R	1	1.90	55.48	39.34	3.28	0
10-25-R	2	0.96	70.15	26.72	2.17	0
10-25-R	3	1.79	56.71	38.06	3.44	0
10-25-R	4	2.79	71.41	23.10	2.70	0
10-25-R	5	1.35	49.56	45.26	3.83	0
9-21-G	1	1.43	57.54	37.66	3.37	0
9-21-G	2	0.88	55.10	40.84	2.68	0.49
9-21-G	3	1.62	58.09	37.98	2.92	0
9-21-G	4	1.72	56.58	38.17	3.52	0
9-21-G	5	1.95	54.84	21.98	21.23	0

APPENDIX 2
 TABLE 1 CONTINUED
 MOLE PERCENT END-MEMBERS

SAMPLE	RUN	SPESS- ARTINE	ALMA- DINE	PYROPE	GROSS- ULAR	ANDRA- DITE
10-26-M	1	3.07	67.64	23.01	5.57	0.70
10-26-M	2	1.98	60.79	32.94	4.29	0
10-26-M	3	1.89	47.59	40.03	6.75	3.73
10-26-M	4	1.97	68.21	26.77	3.05	0
10-26-I	1	1.43	54.69	35.88	7.25	0.74
10-26-I	2	0	10.72	68.03	18.02	3.23
10-26-I	3	1.74	75.47	12.23	3.88	6.68
10-26-I	4	1.66	62.03	29.66	6.66	0
10-27-A	1	1.70	57.34	36.75	4.21	0
10-27-A	2	0	46.83	40.56	8.25	4.36
10-27-A	3	0	57.50	35.28	7.22	0
9-21-B	1	0	56.90	37.10	6.00	0
9-21-B	2	0.82	73.52	22.56	3.10	0
9-21-B	3	1.45	70.39	24.60	3.55	0